Aalto University
School of Engineering

Erik Tollander

Modelling Error of Plywood Beam Constitutive Equation

Master's Thesis
Espoo, 22nd August, 2016

Supervisor: Professor Jukka Tuhkuri, Aalto University
Advisor: Jouni Freund D.Sc (Tech)

Aalto University
School of Engineering
Degree Programme in Mechanical Engineering

ABSTRACT OF
MASTER'S THESIS

Author: Erik Tollander

Title: Modelling Error of Plywood Beam Constitutive Equation

Date:	22nd August, 2016	**Pages:**	viii + 55
Major:	Applied Mechanics	**Code:**	K3006
Supervisor:	Professor Jukka Tuhkuri		
Advisor:	Jouni Freund D.Sc (Tech)		

The constitutive equations of the standard beam model and a refined beam model were compared to find the modelling error in the constitutive equation of the standard beam model. The underlying assumption of the comparison is that the modelling error in the refined model is much smaller than that of the standard one. A cross stacked plywood material with different values of relative material and geometric parameters were used in the comparison. The error was quantified by rigidity correction factors, which can be used to modify the constitutive equation of the standard beam model into the refined one. In stress, the error was quantified by comparing the maximum stress of the standard and the refined models for each loading modes separately.

To replicate wood in a simple but still accurate form, the layers were assumed to be of ideal orthotropic elastic material that is symmetric around one stiffer direction. Plywood was defined as a cross stacked layered material, where the layer angle is altered between normal and transverse direction.

The rigidity correction factors indicate that the plywood beam constitutive equation of the standard model overestimates the rigidity in shear and torsion. However, the standard beam model predicts rigidity correctly in the stretching and bending modes, but underestimates the rigidity when the layup is highly asymmetric. For shear along the plies the standard model requires the well-known stress correction factor of 1.5 (Timoshenko et al., 1970). In the transverse direction to the plies the standard model stress is lower than 1.5 and even overestimated for most plywood applications.

The outcome is that the standard model predicts the maximum normal stress correctly in bending and stretching modes. In torsion the modelling error in maximum shear stress is significant and is highly dependent on the aspect ratio and the orthotropy of the material. The results also shows that none of the rigidity correction factors and neither any of the stress correction factors depends on the material variables for a solid homogeneous orthotropic material, and may therefore be calculated with the same correction factors as isotropic materials.

Keywords: Plywood, veneer, engineered wood, constitutive beam equation, Timoshenko beam model, composite, cross stacked composite, rigidity correction factor, stress correction factor

Language: English

Aalto-universitetet
Högskolan för ingenjörsvetenskaper
Examensprogram för maskinteknik

SAMMANDRAG AV
DIPLOMARBETET

Utfört av: Erik Tollander

Arbetets namn: Balk ekvationens modellfel för Plywood

Datum:	22 augusti 2016	**Sidantal:**	viii + 55
Huvudämne:	Teknisk mekanik	**Kod:**	K3006
Övervakare:	Professor Jukka Tuhkuri		
Handledare:	TkD Jouni Freund		

En jämförelse mellan standard balkmodellens och en förfinad modells konstitutiva ekvationer gjordes för att finna modellfelet som uppstår av de antagandena som är inneboende i standard modellen. Det underliggande antagandet i jämförelsen är att den förfinade modellens inneboende modellfel är avsevärt mindre än standard modellens fel. I jämförelsen användes materialmodellen för krysslimmad faner som plywood där de relativa material och geometriska parametrarna varierades. Felet vid styvhet mättes med hjälp av korrektionsfaktorer för styvhet. Korrektionsfaktorerna för styvhet kan användas för att återskapa den förfinade balkmodellen med hjälp av standard modellen. Felet vid spänning jämfördes den högsta spänningen mellan modellerna för olika belastningar.

För att återge trä som material för faneret, användes en ideell ortotropisk materialmodell vars elastiska egenskaper är symmetriska tvärs en styvare riktning. Plywood definierades som krysslimmad faner, där fanerets fiberriktningen är tvärs det närliggande faneret.

Korrektionsfaktorerna för styvhet gav att standard balkmodellen över estimerar styvheten vid skjuvning och torsion. Vid sträckning och böjning ger standard balkmodellen emellertid korrekt resultat, utom vid extrem asymmetri i laminatet då resultatet är under estimerat. Vid skjuvlast längs faneren krävs den kända korrektionsfaktorn för spänning 1.5 (Timoshenko et al., 1970). Då skjuvlasten är tvärs faneren, så är korrektionsfaktorn för spänning under 1.5 och vid de flesta plywood applikationerna är spänningen rent av över estimerad.

Standard balkmodellen estimerar maximispänningen rätt vid normal last och böj moment. Vid torsion kan konstateras att modellfelet för skjuvspänningen är signifikant och beror till stor utsträckning på materialets ortotropi och på förhållandet mellan tvärsnittshöjd och -bredd. Det kan också konstateras att ingen av korrektionsfaktorerna för styvhet och spänning beror på material parametrarna för ett solitt homogent och ortotropiskt material och kan därför beräknas med samma korrektionsfaktorer som för ett isotropiskt material.

Nyckelord: Plywood, faner, konstitutiv balk ekvation, Timoshenko balkmodell, komposit, krysslaminerad komposit, korrektionsfaktor för styvhet, korrektionsfaktor för spänning

Språk: Engelska

Acknowledgements

I want to thank my supervisor professor Jukka Tuhkuri who gave me the opportunity to write this thesis. I am also grateful towards M.Sc. Avu Huovinen, development manager at Metsä Wood, for showing a deep interest and giving valuable input to my thesis.

My deepest gratitude I have towards my thesis advisor D.Sc Jouni Freund of the Applied Mechanics at Aalto University School of Engineering. D.Sc Freund was of invaluable help during the research and writing of the thesis. He consistently allowed this paper to be my own work, but steered me in the right the direction whenever he thought I needed it.

I would also like to acknowledge all my friends at Teknologföreningen, in Hump Svakar, at Nya Gamla, and all my sailing and music friends who motivated and inspired me in my studies and for giving me a meaningful leisure time.

Finally, I must express my very profound gratitude to my parents for providing me with unfailing support and continuous encouragement throughout my years of study and through the process of researching and writing this thesis. This accomplishment would not have been possible without them. Thank you.

Espoo, 22nd August, 2016

Erik Tollander

Abbreviations and Acronyms

Symbol	Explanation	Förklaring
E_i	Young's modulus	Elastisitetsmodul
G_{ij}	Shear modulus	Skjuvningsmodul
ν_{ij}	Poisson's ratio	Poissons tal
ε_{ij}	Linear strain	Lineär sträckning
σ_{ij}	Stress	Spänning
$\vec{u}$	Deflection of beam	Böjning av balken
$\vec{\theta}$	Rotation of cross section	Rotation av tvärsectionen
$\vec{\varepsilon}$	Strain vector	Sträckningsvektor
$\vec{\kappa}$	Beam curvature vector	Böjningsvektor
α	Relative Young's modulus	Relativ elastisitetsmodul
γ	Relative shear modulus	Relativ sjuvningsmodul
β	Relative Poisson's ratio	Relativ Poisson's tal
δ	Aspect ratio of cross section	Tvärsectionens relativa bredd
n	Number of layers	Skikt antal
b	Width of cross section	Tvärsectionens brädd
h	Height of cross section	Tvärsectionens höjd
t	Layer thickness	lagertjocklek
i	Layer number	Skikt nummer
ϕ	Grain orientation	Ådringens riktning
χ	Rigidity correction factor	Styvhets korrigeringsfaktor
ψ	Stress correction factor	Spänningens korrigeringsfaktor
Ξ	Loading mode	Belastningsmod
$\vec{e}_x, \vec{e}_y, \vec{e}_z$	Unit vectors for beam	Enhetsvektorer för balk
$\vec{e}_1, \vec{e}_2, \vec{e}_3$	Unit vectors for veneer	Enhetsvektorer för skikt
$\overleftrightarrow{E}, \overleftrightarrow{E}$	Elasticity dyad	Elastisitetsdyad
$\overleftrightarrow{I}, \overleftrightarrow{I}$	Identity dyad	Identitetsdyad
FEM	Finite Element Method	Den finita element metoden
RVE	Representative volume element	Representerande material volym element

Contents

List of Tables

List of Figures

1 Introduction

In year 2014 forest industry gross value in Finland was 19.7 billion EUR, which stands for 20.2 % of the total export. In the same year plywood was produced 1160 m^3 of which 87 % was exported. (Puuinfo, 2016) Engineered wood products of layered structure are an important part of the industry. The advantages of the parent wood is inherent in engineered wood, in addition to the enhanced properties of its laminated structure. Wood based material in general has the ability of accommodate short term overloads. The ability to withstand short term overloads are very useful in constructions in areas of seismic activity or cyclonic wind, and it is also of importance when used in flooring or as concrete formwork. The laminated structure of plywood distributes the loads from impact over a larger area on the opposite face, which effectively reduces the tensile stress.

Examples of engineered wood are plywood, laminated veneer lumber (LVL), laminated sawn timber, cross laminated timber (CLT), and oriented strand board (OSB), plywood is cross stacked laminated veneers. Due to high strength and stiffness to weight ratios plywood is cost effective. Example of structural applications are flooring, shear walls, formwork and webbed beams. Plywood remains relatively stable due to temperature and moisture change, because of the cross stacked structure. (Wood Solutions, 2016) LVL consists of laminated veneers, where the major part of the veneers are in the same direction. Laminated sawn timber called Gluelam, is a product where the outer layers are of a higher strength classification, than the inner layers which appear more as a core in a sandwich beam. CLT is very similar to plywood, but is manufactured of sawn timber. Thickness of a single layer in CLT is usually 19 mm, as veneers in plywood are usually below 3 mm. CLT is mostly used as wall and floor elements in building industry.(Puuinfo, 2016) By bonding together thin wood strands with adhesive a structural panel called OSB. The strands of OSB are generally oriented in the same direction on both faces and in the perpendicular direction between them, to obtain for a better dimensional stability. The layup of OSB produces similar material behaviour to plywood and it is stronger than particleboard. (Wood Solutions, 2016) Both Gluelam and LVL are used as slender beams in constructions, such as rafters and pillars (Puuinfo, 2016). The laminated structure of Gluelam and LVL enables a much greater beam span for sawn timber.

Beam models are widely used in the design phase and material tests to find the layer properties out of measurement for wooden plate products (EN 310, 1993; EN 789, 2004). The kinematic assumptions of Euler–Bernoulli beam model states that every cross section remains as a plane and perpendicular to the normal axis of the beam in deformation. The Timoshenko beam theory relaxes the normality assumption of the Euler–Bernoulli beam theory (Reddy et al., 1997), so that the cross section need not to stay perpendicular to the normal axis in deformation. This makes Timoshenko beam model more suitable for short beams and high cross sections, as it takes into account shear deformation. Both beam theories are well suited for beams in bending and in the obvious loading by an axial force.

In shear and torsion, the modelling error in rigidity and stress may be significant.

In torsion, the standard beam model shows great errors for other cross section shapes than a circle and annulus, even for an isotropic material (Freund and Karakoç, 2015). For layered wood applications the kinematic assumptions of the Timoshenko beam model may not be satisfied, which may induce substantial modelling error in torsion and shear loading modes. Quoting (Kennedy and Martins, 2012) "Capturing shear deformation effect is, in general, more important for a composite beam than for a geometrically equivalent isotropic beam, due to the significantly lower ratio of the shear to extension modulus exhibited by composite materials". However, with proper shear, bending, and torsion correction factors the constitutive equation modelling error in rigidity can be reduced. For laminated structures the material properties may vary between layers, which can cause warping modes that are very different from those of a homogeneous isotropic material There may occur stress transverse direction and shear stresses between the layers due to different material behaviour between the layers, which the standard beam model omits.

Since the first appearance of the Timoshenko beam model there has been several suggestions for the shear correction for different beam cross sections of isotropic material (Cowper, 1968; Freund and Karakoç, 2015; Stephen, 1980; Timoshenko, 1921, 1922). Various somewhat different methods used explain the difference of the shear corrections. The shear correction factor for a rectangular cross section for statical loading and far from the boundaries is well known as 5/6 (Gere and Timoshenko, 1984) and can be obtained analytically (Freund and Karakoç, 2015). There are also methods to obtain shear correction factors for laminated beams (Madabhusi-Raman and Davalos, 1996) and anisotropic beam (Pai, 1995).

1.1 Aim and structure of the Study

The aim of this thesis to quantify modelling error of plywood beam constitutive equation. This is done by comparing the constitutive equation of the standard beam model and a refined beam model. The refined beam model presented in this thesis modifies the kinematic assumptions of the standard beam model by including warping displacement in the constitutive equation. The quantification of the error is given by rigidity correction factors, which may be used in the standard beam model to replicate the refined beam model. The difference in stress prediction is also discussed to quantify error in stress. Comparing the maximum stress by the standard and the refined beam model gives the stress correction factor. Knowing the maximum stress enables strength criterion design.

Plywood is defined as a laminated layered material of evenly thick and cross stacked veneers. Cross stacked meaning that the veneer angle of the plies is altering between 0° and 90° between the layers. Wood is assumed to be a linearly elastic orthotropic material, which means that it has three orthogonal planes of symmetry. In addition, the warping is assumed to be free, as there are almost no application for engineered wood with warping restrained. The layup of the laminated plywood material is cross stacked, warping is assumed to be free, and wood is assumed as a linearly elastic ideal orthotropic material. The time dependent material behaviour

as well as the heat and moisture effects of the material are omitted.

In chapter 2 the orthotropic material model is presented, which is used in the simulations. The standard beam theory is presented in chapters 3, including derivation of the plywood beam constitutive equation. A refined beam model for plywood is presented in chapter 4. The refined beam model includes warping of the cross section and is therefore replicating the three dimensional elasticity theory and assuming that warping is not constrained.The simulation experiment is presented in chapter 5. In chapter 6 the rigidity and stress correction factors are analysed and discussed. The outcome of the experiments as well as the scope relevance and possible deficiency of the results are discussed in chapter 7.

1.2 Dyadic Notation

In this thesis the dyadic notation is used. The summation convention is used over repeated indices

$$a_i b_i = \sum_{i \in I} a_i b_i = a_1 b_1 + a_2 b_2 + ... + a_n b_n. \tag{1}$$

A right–arrow over the symbol is the notation for a vector, a double arrow over the symbol for a second order dyad, and two double arrows on top of each other for a fourth order dyad

$$\vec{a} = a_i \vec{e_i}, \tag{2}$$

$$\overleftrightarrow{A} = \vec{e_i} A_{ij} \vec{e_j}, \tag{3}$$

$$\overleftrightarrow{\overleftrightarrow{A}} = \vec{e_i} \vec{e_j} A_{ijkl} \vec{e_k} \vec{e_l} \tag{4}$$

respectively. Bold font symbol, as $\boldsymbol{A}$ is used for matrices. The unit vectors are noted as $\vec{e_i}$ for the i-axis. The second and fourth order identity dyads in a Cartesian xyz– coordinate system are given by

$$\overleftrightarrow{I} = \vec{e}_x \vec{e}_x + \vec{e}_y \vec{e}_y + \vec{e}_z \vec{e}_z, \tag{5}$$

$$\begin{aligned} \overleftrightarrow{\overleftrightarrow{I}} = {} & \vec{e}_x \vec{e}_x \vec{e}_x \vec{e}_x + \vec{e}_y \vec{e}_y \vec{e}_y \vec{e}_y + \vec{e}_z \vec{e}_z \vec{e}_z \vec{e}_z + \vec{e}_x \vec{e}_y \vec{e}_y \vec{e}_x + \vec{e}_y \vec{e}_x \vec{e}_x \vec{e}_y \\ & + \vec{e}_y \vec{e}_z \vec{e}_z \vec{e}_y + \vec{e}_z \vec{e}_y \vec{e}_y \vec{e}_z + \vec{e}_z \vec{e}_x \vec{e}_x \vec{e}_z + \vec{e}_x \vec{e}_z \vec{e}_z \vec{e}_x. \end{aligned} \tag{6}$$

respectively. The conjugate of a second order dyad is

$$\overleftrightarrow{A}^{\mathbf{c}} = \left(\vec{e_i} A_{ij} \vec{e_j} \right)^{\mathbf{c}} = \vec{e_j} A_{ij} \vec{e_i}. \tag{7}$$

For a fourth order dyad there is defined the dyad transpose, the left and right conjugates as

$$\overleftrightarrow{\overleftrightarrow{A}}^{\mathbf{c}} = \left(\vec{e_i} \vec{e_j} A_{ijkl} \vec{e_k} \vec{e_l} \right)^{\mathbf{c}} = \vec{e_k} \vec{e_l} A_{ijkl} \vec{e_i} \vec{e_j}, \tag{8}$$

$$\overleftrightarrow{\overleftrightarrow{A}}_{\mathbf{c}\cdot} = \left(\vec{e_i} \vec{e_j} A_{ijkl} \vec{e_k} \vec{e_l} \right)_{\mathbf{c}\cdot} = \vec{e_j} \vec{e_i} A_{ijkl} \vec{e_k} \vec{e_l}, \tag{9}$$

$$\overleftrightarrow{A}_{\cdot\mathbf{c}} = \left(\vec{e}_i\vec{e}_j A_{ijkl}\vec{e}_k\vec{e}_l\right)_{\cdot\mathbf{c}} = \vec{e}_i\vec{e}_j A_{ijkl}\vec{e}_l\vec{e}_k. \tag{10}$$

The double dot product is defined as

$$\vec{a}\vec{b} : \vec{c}\vec{d} = (\vec{a}\cdot\vec{d})(\vec{b}\cdot\vec{c}). \tag{11}$$

2 Plywood Material

In this chapter the material model used in this study is presented. In section 2.1 the modified elasticity dyad satisfying the beam model assumption is derived from the constitutive equation and the orthotropic material mode. Material parameters of wood is presented in section 2.2. The cross stacked layup of plywood is presented in section 2.3

Microscopical structure of wood is very complex as it consists of cells of different density, geometry, and orientation. Due to the manner in which a tree grows and the arrangement of the wood cells within the stem, wood can be considered locally as an orthotropic material that possesses three principal directions (Holmberg et al., 1999). In figure 1b the RVE of a hexagonal honeycomb is presented. Micro structure of wood is similar to that of the hexagonal honeycomb (Gibson and Ashby, 1997; Jr. and Qing, 2008; Qing and Jr., 2011; Sjölund et al., 2014) Another material with similar material behaviour as wood is fibre composite, as glass or carbon fibre reinforced composite, for which RVE is presented in figure 1c. In the material model, the micro structure is omitted and the elastic properties are associated with a representative volume element (RVE). Figure 1 shows some idealised wood models and one for a heterogeneous orthotropic material.

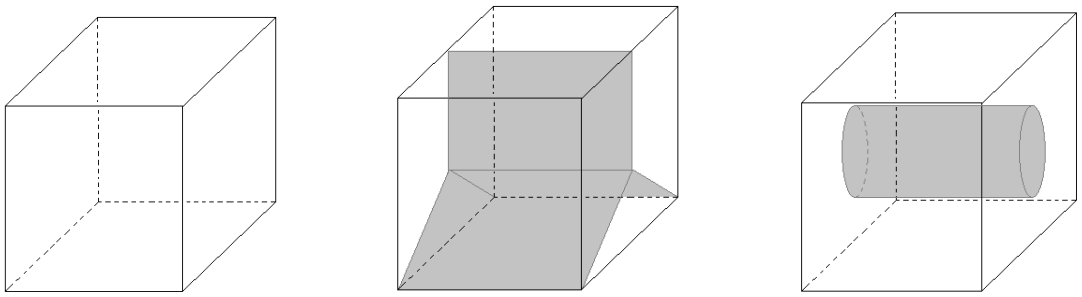

(a) Orthotropic (b) Hexagonal cells (c) Fibre composite

Figure 1: Representative volume element for a heterogeneous orthotropic material (1a), a hexagonal honeycomb structure similar to that of the wood cells in (1b) and a fibrous composite (1c)

2.1 Orthotropic Veneer Model

The constitutive equation for a linearly elastic material found in literature (Gould, 1994; Reddy, 2004), can be written in dyadic notation as

$$\overleftrightarrow{\sigma} = \overleftrightarrow{\overleftrightarrow{E}} : \overleftrightarrow{\varepsilon} = \overleftrightarrow{\overleftrightarrow{E}} : \nabla\vec{u} \tag{12}$$

where $\overleftrightarrow{\sigma}$ is the stress dyad, $\overleftrightarrow{\overleftrightarrow{E}}$ is the elasticity dyad, $\overleftrightarrow{\varepsilon}$ is the strain dyad, and $\nabla\vec{u}$ is the displacement gradient. The displacement gradient can be written in the form

$$\nabla\vec{u} = \frac{1}{2}\left(\nabla\vec{u} + \nabla\vec{u}^{\mathrm{c}}\right) + \frac{1}{2}\left(\nabla\vec{u} - \nabla\vec{u}^{\mathrm{c}}\right) \tag{13}$$

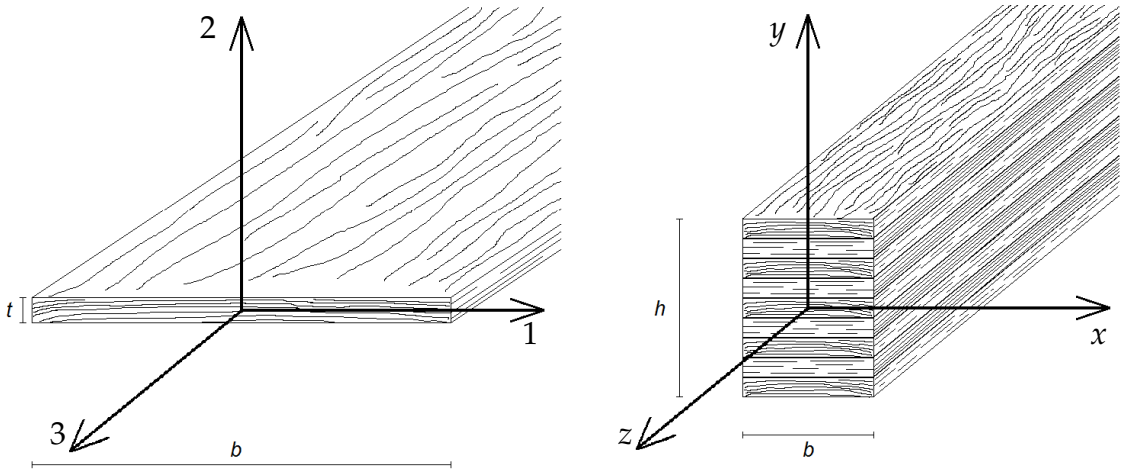

(a) Veneer coordinate system (b) Beam coordinate system

Figure 2: Material and structure coordinate system of plywood beam

where the first term is the deformation, which is symmetric and the second part is the rotation, which is antisymmetric. The second form of equation (12) is valid due to the antisymmetry of the second part of $\nabla\vec{u}$ and the right hand minor symmetry of $\overleftrightarrow{E}$. The elasticity dyad meets the criteria of major symmetry $\overleftrightarrow{E} = \overleftrightarrow{E}^{\mathsf{T}}$, as well as the minor symmetries on both left $\overleftrightarrow{E} = \overleftrightarrow{E}_{\mathbf{c}\cdot}$ and right $\overleftrightarrow{E} = \overleftrightarrow{E}_{\cdot\mathbf{c}}$ side (Schreurs, 2013). Due to the left symmetry of the elasticity dyad the stress dyad $\overleftrightarrow{\sigma}$ is symmetric.

The material properties of a veneer are most convenient to be presented in the orthogonal transverse, radial, and longitudinal directions of the 123 - coordinate system, as shown in 2a. The corresponding basis vectors of the veneer coordinate system are $\vec{e}_1$, $\vec{e}_2$, and $\vec{e}_3$. Veneer is assumed to behave as a homogeneous ideally orthotropic material, which means that plywood can be considered piecewise homogeneous material as veneer angle is different in the layers. The plywood beam is described in xyz - coordinate system as shown in figure 2b, the corresponding base vectors are $\vec{e}_x$, $\vec{e}_y$, and $\vec{e}_z$. Due to the layup of plywood, the veneer and the beam coordinate systems may not coincide. The relationship between the veneer and beam coordinate basis vectors is

$$\begin{Bmatrix} \vec{e}_1 \\ \vec{e}_2 \\ \vec{e}_3 \end{Bmatrix} = \begin{bmatrix} \cos\phi & 0 & -\sin\phi \\ 0 & 1 & 0 \\ \sin\phi & 0 & \cos\phi \end{bmatrix} \begin{Bmatrix} \vec{e}_x \\ \vec{e}_y \\ \vec{e}_z \end{Bmatrix}. \tag{14}$$

where ϕ is the orientation angle of the ply. Figure 3 shows the orientation of the veneer coordinate and beam coordinate systems.

An orthotropic veneer material has three axis of symmetry, which are orthogonal to each other. The material model is given by

$$\begin{Bmatrix} \sigma_{11} \\ \sigma_{22} \\ \sigma_{33} \end{Bmatrix} = \begin{bmatrix} \frac{1}{E_1} & \frac{-\nu_{21}}{E_2} & \frac{-\nu_{31}}{E_3} \\ \frac{-\nu_{12}}{E_1} & \frac{1}{E_2} & \frac{-\nu_{32}}{E_3} \\ \frac{-\nu_{13}}{E_1} & \frac{-\nu_{23}}{E_2} & \frac{1}{E_3} \end{bmatrix}^{-1} \begin{Bmatrix} \varepsilon_{11} \\ \varepsilon_{22} \\ \varepsilon_{33} \end{Bmatrix} = \boldsymbol{E} \begin{Bmatrix} \varepsilon_{11} \\ \varepsilon_{22} \\ \varepsilon_{33} \end{Bmatrix}, \tag{15}$$

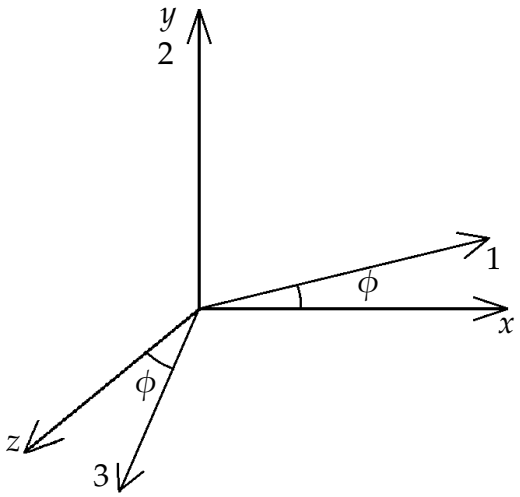

Figure 3: Orientation of coordinate systems

$$\begin{Bmatrix}\sigma_{12}\\ \sigma_{23}\\ \sigma_{31}\end{Bmatrix} = \begin{bmatrix}\frac{1}{G_{12}} & 0 & 0\\ 0 & \frac{1}{G_{23}} & 0\\ 0 & 0 & \frac{1}{G_{31}}\end{bmatrix}^{-1} \begin{Bmatrix}2\varepsilon_{12}\\ 2\varepsilon_{23}\\ 2\varepsilon_{31}\end{Bmatrix} = \boldsymbol{G} \begin{Bmatrix}2\varepsilon_{12}\\ 2\varepsilon_{23}\\ 2\varepsilon_{31}\end{Bmatrix}, \tag{16}$$

where E_i is the Young's modulus along the i-axis, G_{ij} is the shear modulus in the ij-plane, and ν_{ij} is the Poisson's ratio that corresponds to contraction in direction j when an extension is applied in direction of i. The elasticity matrices $\boldsymbol{E}$ and $\boldsymbol{G}$ are symmetric (Reddy, 2004), from which it follows

$$\frac{\nu_{ij}}{E_i} = \frac{\nu_{ji}}{E_j} \qquad i, j \in \{1, 2, 3\}. \tag{17}$$

There are only nine independent material parameters for a orthotropic material, which can be chosen in various ways in equations (15), (16), and (17). Use of the major Poisson's ratios give the opportunity to derive all nine orthotropic parameter from six given. The major Poisson's ratios are defined as the ones that are greater in the equation (17) or

$$\nu_{ij_{major}} = \nu_{ji}\frac{E_i}{E_j} \quad E_i \geq E_j. \tag{18}$$

Comparison of equations (12), (15), and (16) gives the material elasticity dyad as

$$\overleftrightarrow{E} = \begin{Bmatrix}\vec{e}_1\vec{e}_1\\ \vec{e}_2\vec{e}_2\\ \vec{e}_3\vec{e}_3\end{Bmatrix}^{\mathsf{T}} \boldsymbol{E} \begin{Bmatrix}\vec{e}_1\vec{e}_1\\ \vec{e}_2\vec{e}_2\\ \vec{e}_3\vec{e}_3\end{Bmatrix} + \begin{Bmatrix}\vec{e}_1\vec{e}_2 + \vec{e}_2\vec{e}_1\\ \vec{e}_2\vec{e}_3 + \vec{e}_3\vec{e}_2\\ \vec{e}_3\vec{e}_1 + \vec{e}_1\vec{e}_3\end{Bmatrix}^{\mathsf{T}} \boldsymbol{G} \begin{Bmatrix}\vec{e}_2\vec{e}_1 + \vec{e}_1\vec{e}_2\\ \vec{e}_3\vec{e}_2 + \vec{e}_2\vec{e}_3\\ \vec{e}_1\vec{e}_3 + \vec{e}_3\vec{e}_1\end{Bmatrix}. \tag{19}$$

As matrices $\boldsymbol{E}$ and $\boldsymbol{G}$ are symmetric the elasticity dyad satisfies the major and minor symmetries $\overleftrightarrow{E} = \overleftrightarrow{E}^{\mathbf{c}} = \overleftrightarrow{E}_{\mathbf{c}\cdot} = \overleftrightarrow{E}_{\cdot\mathbf{c}}$. Representation of the elasticity dyads of the

veneers in the beam coordinate system are obtained by replacing the basis vectors of the veneer system in equation (19), by their representations in terms of the beam system.

Additional kinematic conditions, like vanishing of some stress components no matter the strain can be satisfied 'a priori' by modifying the elasticity dyad. The kinetic assumption $\sigma_{xx} = \sigma_{yy} = 0$ of the standard Timoshenko beam theory states that normal stresses in all but the beam axial direction vanishes (Timoshenko and Goodier, 1970) constitutive equation (12) gives

$$\sigma_{xx} = \vec{e}_x\vec{e}_x : \overleftrightarrow{E} : \overleftrightarrow{\varepsilon} = 0, \tag{20}$$

$$\sigma_{yy} = \vec{e}_y\vec{e}_y : \overleftrightarrow{E} : \overleftrightarrow{\varepsilon} = 0 \tag{21}$$

from where the strain components ε_{xx} and ε_{yy} can be expressed in terms of the other strain components, ply angle ϕ, and the material parameters of the veneer.

Using the relationships, the strain components ε_x and ε_y can be eliminated from equation (12) to get first the representaion

$$\overleftrightarrow{\underline{\sigma}} = \overleftrightarrow{E} : \overleftrightarrow{\underline{\varepsilon}}, \tag{22}$$

here and in what follows, the underbar is used to describe any modified property that satisfies the standard Timoshenko beam theory assumptions. By mathematical manipulation the modified properties may be placed in the elasticity dyad of the beam model constitutive equation

$$\overleftrightarrow{\sigma} = \overleftrightarrow{\underline{E}} : \overleftrightarrow{\varepsilon} = \overleftrightarrow{\underline{E}} : \nabla\vec{u}, \tag{23}$$

taking the same form as the full/original constitutive equation in equation (12). The components of the modified elasticity dyad are given by

$$\underline{E}_{ijkl} = \frac{\partial \underline{\sigma}_{ij}}{\partial \varepsilon_{kl}} \qquad i, j, k, l \in \{x, y, z\}. \tag{24}$$

The number of independent and non-zero components in the modified elasticity dyad is only six.

The modified elasticity dyad can be expressed as

$$\overleftrightarrow{\underline{E}} = \begin{Bmatrix} \vec{e}_x\vec{e}_y + \vec{e}_y\vec{e}_x \\ \vec{e}_y\vec{e}_z + \vec{e}_z\vec{e}_y \\ \vec{e}_z\vec{e}_x + \vec{e}_x\vec{e}_z \\ \vec{e}_z\vec{e}_z \end{Bmatrix}^{\mathsf{T}} \begin{bmatrix} \underline{E}_{xyyx} & \underline{E}_{xyyz} & 0 & 0 \\ \underline{E}_{yzxy} & \underline{E}_{yzyz} & 0 & 0 \\ 0 & 0 & \underline{E}_{zxzx} & \underline{E}_{zxzz} \\ 0 & 0 & \underline{E}_{zzzx} & \underline{E}_{zzzz} \end{bmatrix} \begin{Bmatrix} \vec{e}_x\vec{e}_y + \vec{e}_y\vec{e}_x \\ \vec{e}_y\vec{e}_z + \vec{e}_z\vec{e}_y \\ \vec{e}_z\vec{e}_x + \vec{e}_x\vec{e}_z \\ \vec{e}_z\vec{e}_z \end{Bmatrix} \tag{25}$$

The expressions of the elasticity dyad components, are given in appendix 1 as functions of the orientation angle and material parameters.

2.2 Material Parameters

Three-point bending (EN 310, 1993) and four-point bending (EN 789, 2004) of plywood beams are the standard test methods to determine the material parameters for plywood. It is specified in the standards that the test results are applicable only for the plywoods of same wood species, strength class, and stacking sequence. (EN 310, 1993; EN 789, 2004) It is noteworthy that the test methods rely on results based on the standard beam model.

Materials are a distribution of different elements with different properties. The average properties of a material is describing the mechanical behaviour accurately. The material parameters are a set of statistical quantities that describes the macro mechanical behaviour of the material. On macro scale the rigidity of a material is given by a good precision by the average material properties and the variation can be omitted. Material parameters can be presented by the mean value and the 5–percentile value (EN 338, 2003) to describe the variation of the material parameters. There is not a consensus about the material parameters for wood as there is variation between test methods (Hofstetter et al., 2005), strength classes (EN 338, 2003), and handbooks (Wood Handbook, 1999).

There are not broadly available wood material parameters in literature and the values are very different between test methods and test specimens (Hofstetter et al., 2005). There is not a consensus about the material parameters for wood as there is variation between test methods (Hofstetter et al., 2005), strength classes (EN 338, 2003), and handbooks (Wood Handbook, 1999). The values differ broadly due to different growth speed and environment and different test methods (Hofstetter et al., 2005). One suggestion for the orthotropic variables $E_1/E_3 \approx 1/30$ for softwood and $E_1/E_3 \approx 1/15$ for hardwood, and $G_{12}/G_{31} \approx 1/20$ for softwood and $G_{12}/G_{31} \approx 1/5$ for hardwood (EN 338, 2003; Wood Handbook, 1999). Another suggestion for the orthotropic variables for wood are $E_1/E_3 \approx 1/20$ and $G_{12}/G_{31} \approx 1/10$ (Holmberg et al., 1999).

Material parameters of the wood species used in Finnish plywood (Veistinen and Pennala, 1997) and steel are given in table 1. The stiffness E_1 and E_2 are almost equal compared to the E_3 as well as the shear stiffness G_{23} and G_{31} compared to G_{12} for wood (Holmberg et al., 1999).

In table 2 the values of the material parameters for strength class D50 for hardwood as well as the strength classes C24 and C35 for softwood according to the standard (EN 338, 2003), is shown beside the regular values for steel found in literature. The letters D and C in the notation used in the standard stands for deciduous and conifer wood respectively, and the number stands for the characteristic value of bending strength in $\mathrm{N\,mm^{-2}}$.

Table 1: Mean values and 5 - percentile characteristic values of the material parameters for steel, birch, spruce and pine. (Hofstetter et al., 2005)

Material	Steel	Birch	Spruce	Pine
$E_{3_{mean}}$[GPa]	210	15.5	11.6	12.5
$E_{3_{0.05}}$[GPa]	—	13.4	4.5	6.1
$E_{1_{mean}}$[GPa]	210	0.93	0.65	0.96
$E_{1_{0.05}}$[GPa]	—	0.83	0.32	0.62
$G_{12_{mean}}$[GPa]	70	0.23	0.05	0.12
$G_{12_{0.05}}$[GPa]	—	0.16	0.01	0.02
$G_{31_{0.05}}$[GPa]	70	1.06	0.71	0.90
$G_{31_{mean}}$[GPa]	—	1.01	0.42	0.44
$\nu_{31_{mean}}$[−]	0.300	0.463	0.516	0.368
$\nu_{31_{0.05}}$[−]	—	0.422	0.223	0.072

Table 2: Material parameters for steel, hardwood class D40, and softwood classes C24 and C35 given in the standard EN338 (EN 338, 2003)

Material	Steel	D50	C24	C35
E_{0mean} [GPa]	210	14	11	13
E_{005}	—	9.4	7.4	8.7
E_{90mean} [GPa]	210	0.93	0.37	0.43
G_{mean} [GPa]	70	0.88	0.69	0.81

2.3 Layup

The layup for the plywood used in this thesis is always cross stacked and the thickness of each ply is equal. The layup of a plywood is defined by layer thickness t, the veneer angle ϕ for each ply , and the number of layers. Both layer thickness and veneer angle may differ from one layer to another. In the present study all the plies are assumed to be of equal thickness and the veneer angle is perpendicular to the layer previous layer. The layups used in this study is presented in appendix 2 .

Numbering of the plies start from surface layer in the negative and increases in the positive direction of the y-axis The cross stacked layup can be written as a series of ply angle as

$$\phi_i = \frac{\pi}{4}\left[1 - (-1)^i\right] \qquad i \in \{1, 2, ..., n\}\,, \tag{26}$$

in which i is the ply number.

The beam coordinate system is chosen to be in the geometric centre of the cross section. The coordinate of the ply centre is calculated by

$$x_i = 0 \qquad i \in \{1, 2, ..., n\} \tag{27}$$

and

$$y_i = -\frac{h}{2} + \frac{t_i}{2} + \sum_{k=1}^{i} t_{k-1} \qquad i \in \{1, 2, ..., n\}\,, \tag{28}$$

where t_i is the thickness of the ith ply, n the total number of layers, and h is the height of the beam cross section.

3 Standard Beam Model

In this chapter the standard beam model is described for plywood beams. In section 3.1 the assumptions of Timoshenko beam model and the definition of the beam theory modified elasticity dyad is presented. A brief derivation of the general beam equations are presented in section 3.2. The constitutive equation for plywood beams are presented and the equation of cross stacked plywood is derived in section 3.3. A simplified form of beam equations for plywood is found in section 3.4.

3.1 Timoshenko Beam Model

The Timoshenko beam theory is the standard model to predict the mechanical behaviour of slender bodies. In what follows, beam is a slender prismatic body defined by the cross section domain $(x, y) \in \Omega$ and the axis domain $z \in Z$. The standard model assumes that cross sections of the beam move as rigid bodies under deformation, and normal stress components in the x and y directions are negligible. The displacement of the beam is

$$\underline{\vec{u}} = \vec{u}_0(z) + \vec{\theta}_0(z) \times \vec{\rho}(x, y) \tag{29}$$

where translation $\vec{u}_0(z)$ and rotation $\vec{\theta}_0(z)$ of a cross section are associated with the reference point $x = y = 0$ and $\vec{\rho}(x, y) = x\vec{e}_x + y\vec{e}_y$ is the relative position vector. The kinetic assumptions

$$\sigma_{xx} = \sigma_{yy} = 0 \tag{30}$$

is taken into account in the modified elasticity dyad of equation (24).

The displacement gradient can be expressed as

$$\nabla\underline{\vec{u}} = \vec{e}_z \left(\vec{\varepsilon} + \vec{\kappa} \times \vec{\rho}\right) - \overleftrightarrow{I} \times \vec{\theta}_0. \tag{31}$$

The strain measures of the standard beam model are

$$\vec{\varepsilon} = \vec{u}_0' + \vec{e}_z \times \vec{\theta}_0, \tag{32}$$

$$\vec{\kappa} = \vec{\theta}_0', \tag{33}$$

in which prime ($'$) indicates the derivative with respect to z.

Combining the constitutive equation (23) and the displacement gradient in equation (31) the expression of stress can be written as

$$\underline{\overleftrightarrow{\sigma}} = \underline{\overleftrightarrow{\overleftrightarrow{E}}} : \left[\vec{e}_z \left(\vec{\varepsilon} + \vec{\kappa} \times \vec{\rho}\right) - \overleftrightarrow{I} \times \vec{\theta}_0\right] = \left(\underline{\overleftrightarrow{\overleftrightarrow{E}}} \cdot \vec{e}_z\right) \cdot \left(\vec{\varepsilon} + \vec{\kappa} \times \vec{\rho}\right). \tag{34}$$

The last term $\overleftrightarrow{I} \times \vec{\theta}_0$ on the right side of equation (31) is antisymmetric and vanishes due to the minor symmetry of the elasticity dyad with respect to the right index pair. The traction acting on a cross section is given by

$$\underline{\vec{\sigma}} = \vec{e}_z \cdot \underline{\overleftrightarrow{\sigma}} = \left(\vec{e}_z \cdot \underline{\overleftrightarrow{\overleftrightarrow{E}}} \cdot \vec{e}_z\right) \cdot \left(\vec{\varepsilon} + \vec{\kappa} \times \vec{\rho}\right), \tag{35}$$

which can be simplified to

$$\underline{\vec{\sigma}} = \underline{\overleftrightarrow{E}} \cdot (\vec{\varepsilon} + \vec{\kappa} \times \vec{\rho}) \,. \tag{36}$$

The modified dyad of the standard beam model $\underline{\overleftrightarrow{E}} = \vec{e}_z \cdot \underline{\overleftrightarrow{E}} \cdot \vec{e}_z$ is given by

$$\underline{\overleftrightarrow{E}} = \begin{Bmatrix} \vec{e}_x \\ \vec{e}_y \\ \vec{e}_z \end{Bmatrix}^{\mathsf{T}} \begin{bmatrix} \underline{E}_{zxxz} & 0 & \underline{E}_{zxzz} \\ 0 & \underline{E}_{zyyz} & 0 \\ \underline{E}_{zzxz} & 0 & \underline{E}_{zzzz} \end{bmatrix} \begin{Bmatrix} \vec{e}_x \\ \vec{e}_y \\ \vec{e}_z \end{Bmatrix}, \tag{37}$$

the components as functions of orientation angle ϕ and the material parameters are given in Appendix 1 .

The beam model modified elasticity dyads $\underline{\overleftrightarrow{E}}_{\parallel}$ and $\underline{\overleftrightarrow{E}}_{\perp}$ for the veneer angles $\theta = 0°$ and $\theta = 90°$, consistent with the orthotropic material model are

$$\underline{\overleftrightarrow{E}}_{\parallel} \equiv G_{31}\vec{e}_x\vec{e}_x + G_{23}\vec{e}_y\vec{e}_y + E_3\vec{e}_z\vec{e}_z, \tag{38}$$

$$\underline{\overleftrightarrow{E}}_{\perp} \equiv G_{31}\vec{e}_x\vec{e}_x + G_{12}\vec{e}_y\vec{e}_y + E_1\vec{e}_z\vec{e}_z. \tag{39}$$

3.2 Beam Equations

The expression of the virtual work for the full elasticity problem, kinematic and kinetic assumption of the beam model, and the principle of virtual work give the beam equations by mathematical manipulations. Internal forces, external distributed volume forces and surface forces are accounted for in the virtual work expression

$$\delta W^{int} = -\int_Z \int_{\Omega(z)} \overleftrightarrow{\sigma}_{\mathrm{c}} : \delta\nabla\vec{u} \, \mathrm{d}A \, \mathrm{d}z \tag{40}$$

and

$$\delta W^{ext} = \int_Z \int_{\Omega(z)} \vec{f} \cdot \delta\vec{u} \, \mathrm{d}A \, \mathrm{d}z + \sum_{\partial Z} \int_{\Omega(z)} \vec{t} \cdot \delta\vec{u} \, \mathrm{d}A, \tag{41}$$

where $\vec{f}$ is the given volume force and $\vec{t}$ the given surface force acting on the end surfaces only.

When expressions (32) and (33) are substituted in equations (40) and (41), virtual work expression of the beam becomes

$$\delta W = \delta W^{int} + W^{ext}, \tag{42}$$

which leads to

$$\delta W = \int_Z \left(- \begin{Bmatrix} \delta\vec{\varepsilon} \\ \delta\vec{\kappa} \end{Bmatrix}^{\mathsf{T}} \cdot \begin{Bmatrix} \vec{F} \\ \vec{M} \end{Bmatrix} + \begin{Bmatrix} \delta\vec{u}_0 \\ \delta\vec{\theta}_0 \end{Bmatrix}^{\mathsf{T}} \cdot \begin{Bmatrix} \vec{f}_g \\ \vec{m}_g \end{Bmatrix} \right) \mathrm{d}z + \sum_{\partial Z} \begin{Bmatrix} \delta\vec{u}_0 \\ \delta\vec{\theta}_0 \end{Bmatrix}^{\mathsf{T}} \cdot \begin{Bmatrix} \vec{F}_g \\ \vec{M}_g \end{Bmatrix}, \tag{43}$$

in which $\vec{f}_g$ and $\vec{m}_g$ are the distributed force and moment in Z, $\vec{F}_g$ and $\vec{M}_g$ are resultant forces and moments acting on the boundaries ∂Z at $x = y = 0$. Work conjugates to $\vec{\varepsilon}$ and $\vec{\kappa}$ in equation (43)

$$\begin{Bmatrix} \vec{F} \\ \vec{M} \end{Bmatrix} = \int_\Omega \begin{Bmatrix} \vec{\underline{\sigma}} \\ \vec{\rho} \times \vec{\underline{\sigma}} \end{Bmatrix} \mathrm{d}A, \tag{44}$$

are resultants of traction $\vec{\sigma}$ defined in (36).

What remains after these steps, is just an exercise on the fundamental lemma of variation calculus and principle of virtual work with expression in equation (43). The outcome is the boundary value problem for the standard Timoshenko beam model

$$\vec{F}' + \vec{f}_g = 0 \quad \text{in } Z, \tag{45}$$

$$\vec{M}' + \vec{e}_z \times \vec{F} + \vec{m}_g = 0 \quad \text{in } Z, \tag{46}$$

$$n\vec{F} - \vec{F}_g = 0 \quad \text{or} \quad \vec{u}_0 - \vec{u}_g = 0 \quad \text{on } Z, \tag{47}$$

$$n\vec{M} - \vec{M}_g = 0 \quad \text{or} \quad \vec{\theta}_0 - \vec{\theta}_g = 0 \quad \text{on } Z, \tag{48}$$

containing as the unknown functions translation $\vec{u}$ and rotation $\vec{\theta}$ of the cross section which depend on the axial coordinate z only. In the boundary conditions, $n = \pm 1$ is the unit outward normal to ∂Z. External forces consists of distributed force $\vec{f}_g$ and moment $\vec{m}_g$ and resultant forces and moments $\vec{F}_g$ and $\vec{M}_g$. Subscript g is the notation for a given quantity.

3.3 Constitutive Equation for Plywood

The force resultant definition in equation (44) gives

$$\begin{Bmatrix} \vec{F} \\ \vec{M} \end{Bmatrix} = \int_\Omega \begin{bmatrix} \overleftrightarrow{\underline{E}} & -\overleftrightarrow{\underline{E}} \times \vec{\rho} \\ -\left(\overleftrightarrow{\underline{E}} \times \vec{\rho}\right)^{\mathbf{c}} & -\vec{\rho} \times \overleftrightarrow{\underline{E}} \times \vec{\rho} \end{bmatrix} \mathrm{d}A \cdot \begin{Bmatrix} \vec{\varepsilon} \\ \vec{\kappa} \end{Bmatrix} = \begin{bmatrix} \overleftrightarrow{\underline{A}} & \overleftrightarrow{\underline{C}} \\ \overleftrightarrow{\underline{C}}^{\mathbf{c}} & \overleftrightarrow{\underline{B}} \end{bmatrix} \cdot \begin{Bmatrix} \vec{\varepsilon} \\ \vec{\kappa} \end{Bmatrix}, \tag{49}$$

when the expression of traction in equation (36) is substituted there. in which $\overleftrightarrow{\underline{A}}$, $\overleftrightarrow{\underline{B}}$, and $\overleftrightarrow{\underline{C}}$ are the stretching, bending and coupling dyads.

As we assume the plies to be homogeneous, each ply can be integrated separately in definition (49) and the stretching, bending and coupling dyads $\overleftrightarrow{\underline{A}}$, $\overleftrightarrow{\underline{B}}$, and $\overleftrightarrow{\underline{C}}$ in equation (49) can be eqxpressed as

$$\overleftrightarrow{\underline{A}} = \int_\Omega \overleftrightarrow{\underline{E}} \, \mathrm{d}A = \sum_{i=1}^{n} \overleftrightarrow{\underline{E}}_i A_i, \tag{50}$$

$$\overleftrightarrow{\underline{B}} = -\int_\Omega \vec{\rho} \times \overleftrightarrow{\underline{E}} \times \vec{\rho} \, \mathrm{d}A = -\sum_{i=1}^{n} \overleftrightarrow{\underline{E}}_i \vdots \overleftrightarrow{J}_i, \tag{51}$$

$$\overleftrightarrow{\underline{C}} = -\int_\Omega \overleftrightarrow{\underline{E}} \times \vec{\rho} \, \mathrm{d}A = -\sum_{i=1}^{n} \overleftrightarrow{\underline{E}}_i \cdot \overleftrightarrow{S}_i, \tag{52}$$

where the area is A_i, the first moments of area is $\overleftrightarrow{S}_i$, and the second moment of area is $\overleftrightarrow{\overleftrightarrow{J}}_i$ for ply i, and defined as

$$A_i = \int_{\Omega_i} 1 \, \mathrm{d}A, \tag{53}$$

$$\overleftrightarrow{\overleftrightarrow{J}}_i = \int_{\Omega_i} \vec{\rho} \times \overleftrightarrow{\overleftrightarrow{I}}^{\mathbf{c}} \times \vec{\rho} \, \mathrm{d}A, \tag{54}$$

$$\overleftrightarrow{S}_i = \int_{\Omega_i} \overleftrightarrow{I} \times \vec{\rho} \, \mathrm{d}A \tag{55}$$

and are purely geometric quantities depending only on the thickness, width and the relative position of the ply

The expressions for a cross stacked plywood of evenly thick plies $t = h/n$, simplify to

$$A_i = b\frac{h}{n}, \tag{56}$$

$$\begin{aligned}\overleftrightarrow{\overleftrightarrow{J}}_i = b\frac{h}{n}\left[\frac{1}{12}\left(\frac{h}{n}\right)^2 + y_i^2\right](-\vec{e}_x\vec{e}_x\vec{e}_z\vec{e}_z + \vec{e}_x\vec{e}_z\vec{e}_z\vec{e}_x + \vec{e}_z\vec{e}_x\vec{e}_x\vec{e}_z - \vec{e}_z\vec{e}_z\vec{e}_x\vec{e}_x) \\ + \frac{h}{n}\frac{b^3}{12}\left(-\vec{e}_y\vec{e}_y\vec{e}_z\vec{e}_z + \vec{e}_y\vec{e}_z\vec{e}_z\vec{e}_y + \vec{e}_z\vec{e}_y\vec{e}_y\vec{e}_z - \vec{e}_z\vec{e}_z\vec{e}_y\vec{e}_y\right),\end{aligned} \tag{57}$$

$$\overleftrightarrow{S}_i = (\vec{e}_z\vec{e}_x - \vec{e}_x\vec{e}_z)\, bh\frac{1}{n}y_i, \tag{58}$$

where b is the width of the beam cross section.

The stretching, coupling, and bending dyads for a cross stacked plywood can be written as

$$\overleftrightarrow{\underline{A}} = bh\frac{1}{n}\left[nG_{31}\vec{e}_x\vec{e}_x + (n_\parallel G_{23} + n_\perp G_{12})\,\vec{e}_y\vec{e}_y + (n_\parallel E_3 + n_\perp E_1)\,\vec{e}_z\vec{e}_z\right], \tag{59}$$

$$\begin{aligned}\overleftrightarrow{\underline{B}} = &-\sum_{i_\parallel}\left[\left(\frac{b}{12}\left(\frac{h}{n}\right)^3 + b\frac{h}{n}y_{i_\parallel}^2\right)(G_{31}\vec{e}_z\vec{e}_z + E_3\vec{e}_x\vec{e}_x) + \frac{h}{n}\frac{b^3}{12}(G_{23}\vec{e}_z\vec{e}_z + E_3\vec{e}_x\vec{e}_x)\right] \\ &-\sum_{i_\perp}\left[\left(\frac{b}{12}\left(\frac{h}{n}\right)^3 + b\frac{h}{n}y_{i_\perp}^2\right)(G_{31}\vec{e}_z\vec{e}_z + E_1\vec{e}_x\vec{e}_x) + \frac{h}{n}\frac{b^3}{12}(G_{12}\vec{e}_z\vec{e}_z + E_1\vec{e}_x\vec{e}_x)\right],\end{aligned} \tag{60}$$

$$\overleftrightarrow{\underline{C}} = -bh\frac{1}{n}\left(E_3\sum_{i_\parallel} y_{i_\parallel} + E_1\sum_{i_\perp} y_{i_\perp}\right)\vec{e}_z\vec{e}_x, \tag{61}$$

in which $n_\parallel$ is the number of parallel and $n_\perp$ is the number of transverse layers to the beam axis, with veneer angles 0° and 90° respectively. The equations (59),

(61), and (60) will be used as reference to evaluate the shear correction factors for plywood.

If $E_1 = E_2 = E_3 = E$ and $G_{12} = G_{23} = G_{31} = G$, equations (59), (61), and (60) simplify to

$$\overleftrightarrow{\underline{A}} = GA\left(\vec{e}_x\vec{e}_x + \vec{e}_y\vec{e}_y\right) + EA\vec{e}_z\vec{e}_z, \tag{62}$$

$$\overleftrightarrow{\underline{C}} = 0, \tag{63}$$

$$\overleftrightarrow{\underline{B}} = EI_x\vec{e}_x\vec{e}_x + EI_y\vec{e}_y\vec{e}_y + G\left(I_x + I_y\right)\vec{e}_z\vec{e}_z, \tag{64}$$

where the moments of areas $A,\ I_y,\ I_x$ are the integrals of $1,\ x^2$, and y^2 over the cross section Ω, respectively.

3.4 Simplified Form for Plywood Calculations

With a plywood beam of rectangular cross section, the material coordinate system origin at the geometrical centroid the stretching, bending, and coupling dyads take the forms

$$\overleftrightarrow{\underline{A}} = \underline{A}_{11}\vec{e}_x\vec{e}_x + \underline{A}_{22}\vec{e}_y\vec{e}_y + \underline{A}_{33}\vec{e}_z\vec{e}_z, \tag{65}$$

$$\overleftrightarrow{\underline{B}} = \underline{B}_{11}\vec{e}_x\vec{e}_x + \underline{B}_{22}\vec{e}_y\vec{e}_y + \underline{B}_{33}\vec{e}_z\vec{e}_z, \tag{66}$$

$$\overleftrightarrow{\underline{C}} = \underline{C}_{31}\vec{e}_z\vec{e}_x. \tag{67}$$

The strain measures in the generic expressions

$$\vec{\varepsilon} = \varepsilon_x\vec{e}_x + \varepsilon_y\vec{e}_y + \varepsilon_z\vec{e}_z, \tag{68}$$

$$\vec{\kappa} = \kappa_x\vec{e}_x + \kappa_y\vec{e}_y + \kappa_z\vec{e}_z, \tag{69}$$

and their work conjugates

$$\vec{F} = Q_x\vec{e}_x + Q_y\vec{e}_y + N\vec{e}_z, \tag{70}$$

$$\vec{M} = M_x\vec{e}_x + M_y\vec{e}_y + T\vec{e}_z. \tag{71}$$

With these component representations, constitutive equation in equation (49) can be written in the matrix form

$$\begin{Bmatrix} Q_x \\ Q_y \\ N \\ M_x \\ M_y \\ T \end{Bmatrix} = \begin{bmatrix} \underline{A}_{11} & 0 & 0 & 0 & 0 & 0 \\ 0 & \underline{A}_{22} & 0 & 0 & 0 & 0 \\ 0 & 0 & \underline{A}_{33} & \underline{C}_{31} & 0 & 0 \\ 0 & 0 & \underline{C}_{31} & \underline{B}_{11} & 0 & 0 \\ 0 & 0 & 0 & 0 & \underline{B}_{22} & 0 \\ 0 & 0 & 0 & 0 & 0 & \underline{B}_{33} \end{bmatrix} \begin{Bmatrix} \varepsilon_x \\ \varepsilon_y \\ \varepsilon_z \\ \kappa_x \\ \kappa_y \\ \kappa_z \end{Bmatrix}. \tag{72}$$

For symmetric layups, $\underline{C}_{31} = 0$ and the stretch and bending modes are not connected in the constitutive equation. For an asymmetric layup, orthotropic material and the placing of the origin at the geometrical centroid, $\underline{C}_{31} \neq 0$. The coupling term $\underline{C}_{31}$ can be eliminated by moving the origin of the coordinate system along the y-

axis, but with the expense of inducing coupling between shear and torsion $\underline{C}_{13} \neq 0$ instead.

If the layup is symmetric and $N = 0$, the constitutive equation simplifies to

$$\begin{Bmatrix} Q_x \\ Q_y \\ M_x \\ M_y \\ T \end{Bmatrix} = \begin{bmatrix} \underline{A}_{11} & 0 & 0 & 0 & \\ 0 & \underline{A}_{22} & 0 & 0 & 0 \\ 0 & 0 & \underline{B}_{11} & 0 & 0 \\ 0 & 0 & 0 & \underline{B}_{22} & 0 \\ 0 & 0 & 0 & 0 & \underline{B}_{33} \end{bmatrix} \begin{Bmatrix} \varepsilon_x \\ \varepsilon_y \\ \varepsilon_z \\ \kappa_x \\ \kappa_y \\ \kappa_z \end{Bmatrix}, \tag{73}$$

taking into account $N = 0$ 'a priori'. This simplification is also used for slightly non–symmetric layups, which may induce additional modelling error. In cases where $N = 0$ this can be avoided by replacing the bending stiffness by $\chi^*_{33}\underline{B}_{11}$, giving

$$\begin{Bmatrix} Q_x \\ Q_y \\ M_x \\ M_y \\ T \end{Bmatrix} = \begin{bmatrix} \underline{A}_{11} & 0 & 0 & 0 & 0 \\ 0 & \underline{A}_{22} & 0 & 0 & 0 \\ 0 & 0 & \chi^*_{33}\underline{B}_{11} & 0 & 0 \\ 0 & 0 & 0 & \underline{B}_{22} & 0 \\ 0 & 0 & 0 & 0 & \underline{B}_{33} \end{bmatrix} \begin{Bmatrix} \varepsilon_x \\ \varepsilon_y \\ \kappa_x \\ \kappa_y \\ \kappa_z \end{Bmatrix}. \tag{74}$$

When the layup is asymmetric and the coupling is simply omitted, in which the correction factor of the bending stiffness

$$\chi^*_{33} = 1 - \frac{\underline{C}^2_{31}}{\underline{B}_{11}\underline{A}_{33}}, \tag{75}$$

is smaller or equal to one. Therefore, use of equation (73) means exaggerated bending stiffness. Assuming the shear effects to be negligible, the transverse displacement is at some point directly proportional to the bending stiffness and the correction factor also gives a measure of error in the transverse displacement.

4 Refined Beam Theory

The kinematic assumption of the Timoshenko beam is that the planes transverse to the beam longitudinal axis remain planes and move as rigid bodies when the beam is loaded. The quite sever kinematic assumptions is a source for modelling error in rigidity and stress. For example, the standard beam model predicts a piecewise constant shear stress, which may show jumps inside cross section. Also, the zero stress conditions on a unloaded surface is not satisfied, which is against the balance of momentum. The normal strain distribution in the axial direction by the standard beam theory is linear, which is a good approximation for isotropic materials. However, the standard beam theory does not count for the Poisson effect according to which a stress in one direction will impact the strains in the transverse directions. Due to the veneer orthotropic character, the Poisson's ratios may differ between the layers in plywood and therefore there will appear shear stresses close to the veneer interfaces, which are not present in isotropic materials. The standard beam theory is known to have errors especially for laminates (El Fatmi, 2007).

The refined beam model for plywood, used in the simulations of this thesis is based on the model by Freund and Karakoç (2015). The main idea and equations are described in section 4.1. In section 4.2 the general methodology of finite element simulations are briefly described. Warping and stresses of plywood beam cross section of the standard and the refined beam models are presented in section 4.3.

4.1 Two–scale beam model

The standard beam theory is based on the linear elasticity theory and additional assumptions, concerning displacement and stress in equations (29) and (30). Reduction of the modelling error of the standard beam model means modifications of these assumptions into a less severe direction. In the uniform warping model, equation (29) is replaced by

$$\vec{u} = \underline{\vec{u}} + \Delta\vec{u}, \tag{76}$$

in which $\Delta\vec{u}(x, y, z)$ is the warping displacement, and $\underline{\vec{u}}$ is the standard beam model displacement in equation (29). The kinetic assumption, in equation (30) is omitted in the refined model, which means that the elasticity dyad $\overleftrightarrow{E}$ in equation (19), without any modifications, is used in the refined beam model. The warping displacement part is taken to be

$$\Delta\vec{u} = \overleftrightarrow{u}_{\varepsilon} \cdot \vec{\varepsilon} + \overleftrightarrow{u}_{\kappa} \cdot \vec{\kappa}, \tag{77}$$

which is linear in the strain measures of the standard beam model. The stress of the refined beam model is calculated by combining the constitutive equation (12) and the refined beam model kinematic assumption in equation (76) as

$$\overleftrightarrow{\sigma} = \overleftrightarrow{E} : \nabla \left(\underline{\vec{u}} + \Delta\vec{u} \right). \tag{78}$$

The minimum potential energy principle of mechanics is used to determine the warping displacement part. By considering the strain energy only, warping displacement gives a stationary value of the functional

$$\Pi\left(\Delta\vec{u},\vec{\lambda}\right)=\frac{1}{2}\int_{\Omega}\overleftrightarrow{\sigma}^{\mathbf{c}}\mathbf{:}\nabla\vec{u}\,\mathrm{d}A-\int_{\Omega}\vec{\lambda}\cdot\Delta\vec{u}\,\mathrm{d}A, \tag{79}$$

where Ω is the domain occupied by the cross section, $\vec{\lambda}$ is a Lagrange multiplier of same form as $\vec{\underline{u}}$, and the strain measures $\vec{\varepsilon}$ and $\vec{\kappa}$ in equations (32), (33) are considered constants. The Lagrange multiplier term enforces the warping displacement to be orthogonal to $\vec{\underline{u}}$ and ensures uniqueness of decomposition in equation (76).

Equations associated with translation and rotation of the standard model part in equation (78) with equations (44) to (48), the only difference being in the stress expression. The stress resultant definition of the refined beam model can be written as

$$\begin{Bmatrix}\vec{F}\\ \vec{M}\end{Bmatrix}=\int_{\Omega}\begin{Bmatrix}\vec{\sigma}\\ \vec{\rho}\times\vec{\sigma}\end{Bmatrix}\mathrm{d}A=\begin{bmatrix}\overleftrightarrow{A} & \overleftrightarrow{C}\\ \overleftrightarrow{C}^{\mathbf{c}} & \overleftrightarrow{B}\end{bmatrix}\cdot\begin{Bmatrix}\vec{\varepsilon}\\ \vec{\kappa}\end{Bmatrix}. \tag{80}$$

in which the traction is defined as $\vec{\sigma}=\vec{e}_z\cdot\overleftrightarrow{\sigma}$. The refined beam model constitutive equation (80) is of the same form as the standard model equation (49). The difference between the constitutive equations of the standard and refined models is in the stretching, bending, and coupling dyads $\overleftrightarrow{A}$, $\overleftrightarrow{B}$, and $\overleftrightarrow{C}$. By assuming that the modelling error of the refined model is substantially smaller than the standard model, modelling error in rigidity is given by the difference between the dyads.

4.2 Finite Element Method

An in–house Mathematica code is used to find the stationary point to the functional in equation (79) by the finite element method. An unstructured mesh of triangular elements with a piecewise quadratic polynomial approximation is used. When the approximation, containing the nodal displacements for the warping part, is substituted into functional (79) the outcome is a function, whose stationary requires that all partial derivatives with respect to the nodal displacement vanish. The outcome is a linear equations system for the nodal displacements.

The solver finds the warping modes in equation (77) by giving the value one to each of the strain measures ε_x, ε_y, ε_z, κ_x, κ_y, and κ_z, at a time separately. After that the relationship in equation (79) follows from linearity with respect to the strain measures.

The precision goal of the numerical calculations is three significant figures for the rigidity and stress correction factors. Convergence of the simulations was verified by increasing the number of elements for a few layups of the setting. Stress was found to be more sensitive to the mesh resolution than rigidity, the significance was the greatest for torsion. The precision goal was not achieved in all cases for the stress correction factors.

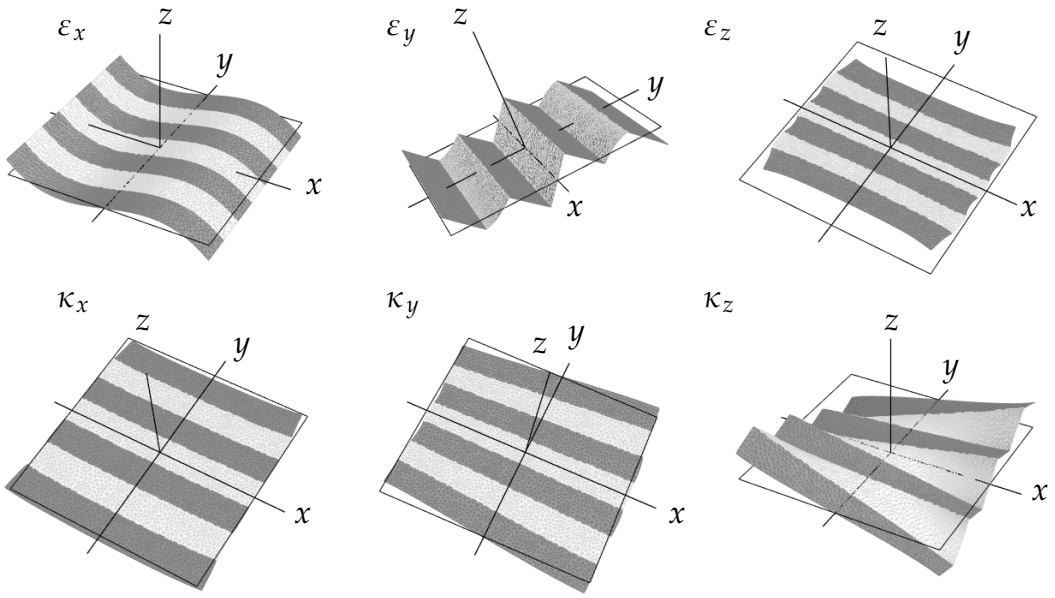

Figure 4: Warping of a seven layer cross stacked plywood beam cross section

4.3 Warping and Stress of a Square Cross Section

The warping and the stress of a seven-layer plywood beam cross section is presented in this section. The purpose is to show some typical results for a plywood material and discuss the modelling error in the standard beam model qualitatively before a more detailed study. The elasticity modules were chosen as $E_3 = 1$, $E_1 = E_2 = 1/10$ the shear modules as $G_{31} = G_{32} = 1$, $G_{12} = 1/20$, and the Poisson's ratios as $\nu_{21} = 1/3$, $\nu_{31} = \nu_{32} = 1/6$ for the veneers, which fairly good represents the relative material parameters for birch in table 1.

Figure 4 shows the warping modes for a seven-layer plywood associated with the shear strain measures ε_x, ε_y, and $\varepsilon_z$on the first row in the same order and κ_x, κ_y, κ_z on the second row in the same order. The box of black line shown in figure 4 is the standard model cross section warping, which is zero. The longitudinal $\phi = 0°$ and transverse $\phi = 90°$ plies are indicated by the dark and light colour, respectively. The warping modes for ε_x, ε_y, and $\kappa_z$are out of plane modes, whereas in the ε_z, κ_x, and $\kappa_z$modes there is only in-plane differences to the standard beam model. The effects of the layered structure and the difference in material properties between the layers is obvious in the modes for shear strain ε_y, normal strain ε_z, and torsional angle κ_z. The veneer material seems not to have effect on the warping due to shear ε_x. For shear ε_y, a much greater local shearing is induced in the less stiff light layers than in the stiffer dark layers. The Poisson effects is clear in the axial stretching ε_z mode of the beam. The axially stiffer dark layers shrinks transversely as they are stretched, whereas the light transversely stiffer layers resist the shrinkage. For bending κ_x, the shrinkage increases in the positive y-direction and extends in the other. There is no obvious material dependent warping for

bending κ_y. For torsion strain κ_z, the shearing for the less stiff light layers are much greater than for the stiffer dark layers. The shear is also much greater in the corners of the cross section and seems to vanish at the x and y axis.

Figures 5 and 6 show the stress components when the beam cross section is loaded by each of the stress resultants Q_x, Q_y, N, M_x, M_y, and T. The refined model prediction is shown in figure 5 and standard model prediction in 6. Vanishing stresses are in gray, positive stress is indicated by a colour between red and gray so that the maximum value is clear red, negative stress is indicated by a colour between blue and gray. On each row the scale is the same, whereas it may differ between rows. For shear force Q_x the refined model gives a continuous shear stress τ_{zx} and no other stresses. The shear force Q_y results in a continuous shear stresses τ_{yz}. The stiffer plies carry most of the axial force N and the bending moments M_x and M_y by axial stress σ_{xx}, the other stresses being insignificant for these loading modes. Axial force N, induces a piecewise constant and the bending moments M_x and M_y a piecewise linear stress distribution, with clearly higher values for the stiffer longitudinal veneers. For torsion T, the shear stress distributions for both τ_{yz} and τ_{zx} are both continuous. Shear stress τ_{yz} reaches greater intensity in the longitudinal than in the transverse veneers, reaching greater absolute values closer to the vertical center and an increasing distance to the centre of the cross section. Shear stress τ_{zx} cyclically increases throughout the stiffer layers from minimum at the bottom to maximum at the top edge.

Stresses for the loading cases N, M_x, and M_y are very similar between the standard and the refined beam model. For the shear force Q_y the standard beam theory gives a uniform shear stress τ_{zx}, throughout the cross section, whereas shear stress by the refined model vanishes at the free unloaded edges and attains its maximum at the horizontal center line. For shear force Q_x the standard model shear stress τ_{yz} is piecewise constant through the cross section and discontinuous at the layer surface, whereas the refined model gives a continuous distribution vanishing at the horizontal surfaces and reaching its maximum at the vertical centreline. Torsion induces a piecewise linear stress distribution for the shear stress τ_{yz} and a linear for the τ_{zx}, getting the minimum at the left and the maximum at the right surface in the longitudinal veneers for τ_{yz}. for $\tau_{zx}$the maximum is at the upper and minimum at the bottom surface.

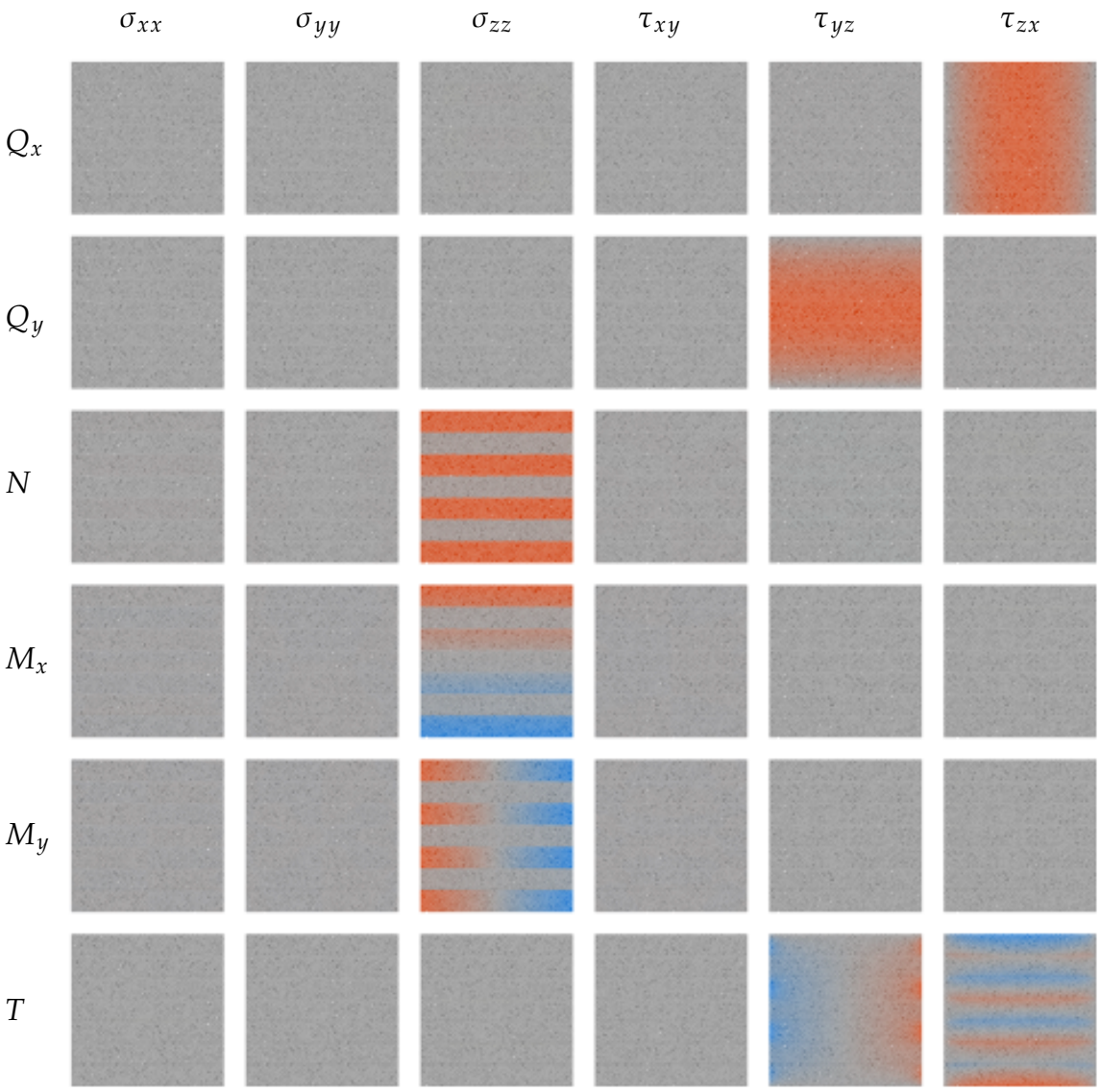

Figure 5: Stress components for a seven layer cross stacked plywood beam

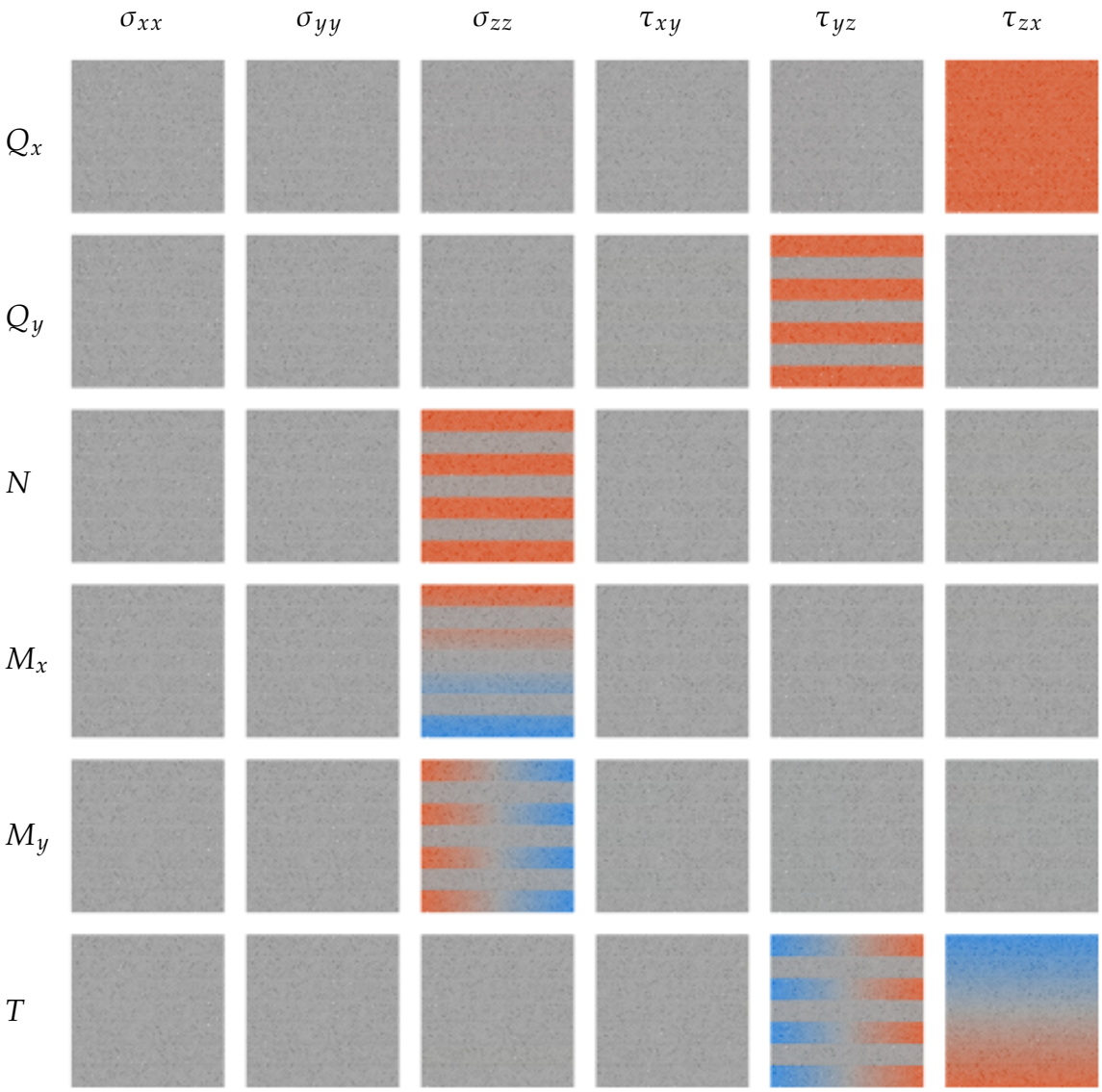

Figure 6: Standard beam model stress components for a seven-layer cross stacked plywood

5 Correction Factors

For a more quantitative picture about the modelling error of the standard constitutive equation, the geometric and material parameters were varied as independent variables of a simulation experiment. The dependent variables were the difference between the standard and the refined model in rigidity and the maximum stress. Rigidity correction factors can be used to modify the constitutive equation of the standard model into the refined one. The rigidity correction factors are also direct measures of the modelling error in the constitutive equations. For a more precise picture about the error in stress the maximum stresses of the different loading modes of the refined and the standard models are compared, giving the stress correction factor.

The design of the simulation experiment and the independent variables are explained in section 5.1. The results of the simulations and the definition of the rigidity correction factors are presented in section 5.2 and the stress correction factors in section 5.3. The outcome of the simulations is used later to discuss the error in the constitutive equation of the standard beam model.

5.1 Material and Method

The veneer material model used in the simulations is defined in equation (15) and (16), where $E_3 = E$ is the elasticity modulus in the strong axis of the ply, $G_{31} = G_{32} = G$ is the shear modulus in the plane of the strong axis, and $\nu_{21} = \nu$ is the Poisson's ratio in the transverse plane to the strong axis. The relative modulus of elasticity, the relative Poisson's ratio, and the relative shear modulus defined by

$$\alpha = \frac{E_1}{E_3} = \frac{E_2}{E_3}, \tag{81}$$

$$\beta = \frac{\nu_{31}}{\nu_{21}} = \frac{\nu_{32}}{\nu_{21}}, \tag{82}$$

$$\gamma = \frac{G_{12}}{G_{23}} = \frac{G_{12}}{G_{31}}, \tag{83}$$

are the independent material variables of the simulation experiment. The aspect ratio and the number of layers

$$\delta = \frac{b}{h}, \tag{84}$$

$$n \in \mathbb{N}, \tag{85}$$

are the independent geometrical variables of the simulation experiment.

The domains used in the simulations are shown in table 3. The values of the independent material variables describe a range of materials from perfectly isotropic to highly orthotropic. Isotropic material is given by the values $\alpha = \beta = \gamma = 1$ and $G = E/(2 + 2\nu)$. Material parameter values $\alpha \approx 1/30,\ \beta \approx 1/2,\ \gamma \approx 1/20$ for spruce and values $\alpha \approx 1/15,\ \beta \approx 1/2,\ \gamma \approx 1/5$ for birch belong to the domains of table 3.

Table 3: Values of the independent dimensionless variables

Variable	Value set
α	{1, 1/2, 1/5, 1/10, 1/20, 1/30}
β	{1, 1/2, 1/5, 1/20, }
γ	{1, 1/2, 1/5, 1/10, 1/20, 1/50}
δ	{1/2, 1, 2, }
n	{1, 2, 3, 4, 7, 8, 15, 16, 21, 24, 30, 31, 35, 36}

In the direction of orthotropy the extreme values of the independent variables are $\alpha = 1/30$, $\beta = 1/20$, $\gamma = 1/50$.

Expressions in equations (81), (82), and (83) give the orthotropic material model in equation (19), with

$$\boldsymbol{E} = E \begin{bmatrix} \frac{1}{\alpha} & -\frac{\nu}{\alpha} & -\beta\nu \\ -\frac{\nu}{\alpha} & \frac{1}{\alpha} & -\beta\nu \\ -\beta\nu & -\beta\nu & 1 \end{bmatrix}^{-1}, \tag{86}$$

$$\boldsymbol{G} = G \begin{bmatrix} \frac{1}{\gamma} & 0 & 0 \\ 0 & 1 & 0 \\ 0 & 0 & 1 \end{bmatrix}^{-1}, \tag{87}$$

which are subjected to kinetic assumptions in equation (30) in the beam model application.

5.2 Rigidity Correction Factors

The rigidity correction matrix

$$\chi = \begin{bmatrix} \chi_{\boldsymbol{A}} & \chi_{\boldsymbol{C}} \\ \chi_{\boldsymbol{C}}{}^{\mathsf{T}} & \chi_{\boldsymbol{B}} \end{bmatrix} = \begin{bmatrix} \underline{\boldsymbol{A}} & \underline{\boldsymbol{C}} \\ \underline{\boldsymbol{C}}^{\mathsf{T}} & \underline{\boldsymbol{B}} \end{bmatrix}^{-1/2} \begin{bmatrix} \boldsymbol{A} & \boldsymbol{C} \\ \boldsymbol{C}^{\mathsf{T}} & \boldsymbol{B} \end{bmatrix} \begin{bmatrix} \underline{\boldsymbol{A}} & \underline{\boldsymbol{C}} \\ \underline{\boldsymbol{C}}^{\mathsf{T}} & \underline{\boldsymbol{B}} \end{bmatrix}^{-1/2} \tag{88}$$

is considered as the dependent variable of the simulation experiment. The matrix is a measure of the difference between the constitutive equations of the refined and the standard beam models. For a symmetric representation, the standard model stiffness matrix is separated into square root inverse matrices on the left and the right hand sides. The inverse square of the rigidity correction matrix exists, as the stiffness matrix of the standard model is positive definite (Kreyszig, 2006). It is obvious from definition in equation (88) that the rigidity correction matrix is a unit matrix, if the constitutive equation of the refined and standard model coincides.

Assuming that the origin of the coordinate system is at the geometric center of

the cross section, the rigidity correction matrix is of the form

$$\boldsymbol{\chi} = \begin{bmatrix} \chi_{11} & 0 & 0 & 0 & 0 & 0 \\ 0 & \chi_{22} & 0 & 0 & 0 & 0 \\ 0 & 0 & \chi_{33} & \chi_{34} & 0 & 0 \\ 0 & 0 & \chi_{34} & \chi_{44} & 0 & 0 \\ 0 & 0 & 0 & 0 & \chi_{55} & 0 \\ 0 & 0 & 0 & 0 & 0 & \chi_{66} \end{bmatrix}, \tag{89}$$

where χ_{11} and χ_{22} are the shear correction factors in the x and y directions, χ_{66} is the torsion correction factor, χ_{33} is the stretch correction factor, and χ_{44} and χ_{55} are the bending correction factors in the x and y directions, respectively. The coupling correction factor between the bending and the stretching modes is χ_{34}. The rigidity correction matrix can be considered as a generalisation of the well known shear and torsion correction factors to the generic loading of a beam.

The constitutive equations of the refined and the standard beam models, and the rigidity correction matrix are related by

$$\begin{Bmatrix} \boldsymbol{F} \\ \boldsymbol{M} \end{Bmatrix} = \begin{bmatrix} \boldsymbol{A} & \boldsymbol{C} \\ \boldsymbol{C}^{\mathsf{T}} & \boldsymbol{B} \end{bmatrix} \begin{Bmatrix} \boldsymbol{\varepsilon} \\ \boldsymbol{\kappa} \end{Bmatrix} = \begin{bmatrix} \underline{\boldsymbol{A}} & \underline{\boldsymbol{C}} \\ \underline{\boldsymbol{C}}^{\mathsf{T}} & \underline{\boldsymbol{B}} \end{bmatrix}^{1/2} \begin{bmatrix} \boldsymbol{\chi}_{\boldsymbol{A}} & \boldsymbol{\chi}_{\boldsymbol{C}} \\ \boldsymbol{\chi}_{\boldsymbol{C}}{}^{\mathsf{T}} & \boldsymbol{\chi}_{\boldsymbol{B}} \end{bmatrix} \begin{bmatrix} \underline{\boldsymbol{A}} & \underline{\boldsymbol{C}} \\ \underline{\boldsymbol{C}}^{\mathsf{T}} & \underline{\boldsymbol{B}} \end{bmatrix}^{1/2} \begin{Bmatrix} \boldsymbol{\varepsilon} \\ \boldsymbol{\kappa} \end{Bmatrix} \tag{90}$$

and therefore the constitutive equation of the refined model can be obtained by the by using the constitutive equation of the standard model and the rigidity correction matrix.

The dependency of the rigidity correction factors on the independent variables in equations (81) to (84) are summarised in table 4.

The logical expressions indicate whether the rigidity correction factors on the rows are affected by the independent variables on the columns. True means that the rigidity correction factor is affected by the independent variable, no matter what, and false that it is not affected. A logical expression defines the condition under which an independent variable affects a rigidity correction factor. Table 4 indicates, for example, that the number of layers for stretch and bending correction factors χ_{33}, , χ^*_{33}, and χ_{44} are not affected by the independent variables when the layup is symmetric, even for values of the relative elasticity modulus different from one i.e. $\alpha \neq 1$. Torsion correction factor χ_{66} is the only rigidity correction factor depending on more than two of the independent variables. It is also the only rigidity correction factor depending on the aspect ratio δ of the beam cross section. Shear correction factor χ_{11} and bending correction factor χ_{55} are found not to depend on the independent variables. Remarkable is that none of the rigidity correction factors depend on the relative Poisson's ratio β.

Table 4: Effect of the independent variables on the rigidity correction factors

	n	α	β	γ	δ
χ_{11}	false	false	false	false	false
χ_{22}	$\gamma \neq 1$	false	false	$n > 1$	false
χ_{33}	$\alpha \neq 1$	$n_{\parallel} = n_{\perp}$	false	false	false
$\chi_{34} = \chi_{43}$	$\alpha \neq 1$	$n_{\parallel} = n_{\perp}$	false	false	false
χ_{44}	$\alpha \neq 1$	$n_{\parallel} = n_{\perp}$	false	false	false
χ_{55}	false	false	false	false	false
χ_{66}	$\gamma \neq 1$	false	false	$n > 1$	true
χ^*_{33}	$\alpha \neq 1$	$n_{\parallel} = n_{\perp}$	false	false	false

The correction factors χ_{22}, χ_{33}, χ_{34}, χ_{66}, χ^*_{33} obtained for the domains in table 3 are given in tables 5, 6, 7, 8, 9, and 10. The shear correction factor χ_{11} was found to be 5/6 no matter the independent variables. Table 5 shows the values of the other shear correction factor χ_{22}. The value depends on the relative shear modulus γ and the number of layers n, as indicated in table 4.

The values of the stretch correction factors χ_{33} are presented in table 6 and the coupling correction factor between stretching and bending modes is presented in table 7. Bending correction factors χ_{44} is presented in table 8. The other bending correction factor χ_{55} is found to be equal to one no matter the independent variables.

The rigidity correction factors χ_{33}, χ_{34}, χ_{43}, and χ_{44} depend on the relative elasticity modulus α and number of layer n, as shown in table 4.

Torsion correction factor χ_{66} is presented in table 9. The torsion correction factor depends on the relative shear modulus γ, the aspect ratio δ, and the number of layers n.

The asymmetry correction factor χ^*_{33} describes the error due to omitting the coupling dyad in the constitutive equation. Omitting the coupling dyad disconnects the stretch and bending modes and simplifies the solving of a beam problem, but induces modelling error if n is even. The asymmetry correction factor χ^*_{33} defined in equation (75) depends on the relative elasticity modulus α. The results for χ^*_{33} are shown in table 10. All the odd number of layers are omitted as $\chi^*_{33} = 1$ for all the symmetrical layups.

Table 5: Shear correction factor χ_{22} as a function of the number of layers n and the relative shear modulus γ

n	γ				
	1	1/5	1/10	1/20	1/50
1	0.833	0.833	0.833	0.833	0.833
3	0.833	0.342	0.191	0.101	0.0421
7	0.833	0.419	0.244	0.132	0.0556
15	0.833	0.443	0.261	0.142	0.0601
21	0.833	0.449	0.265	0.145	0.0612
31	0.833	0.453	0.268	0.147	0.0621
35	0.833	0.454	0.269	0.147	0.0624
2	0.833	0.463	0.276	0.151	0.0641
4	0.833	0.463	0.276	0.151	0.0641
8	0.833	0.463	0.276	0.151	0.0641
16	0.833	0.463	0.276	0.151	0.0641
24	0.833	0.463	0.276	0.151	0.0641
30	0.833	0.463	0.276	0.151	0.0641
36	0.833	0.463	0.276	0.151	0.0641

Table 6: Stretch correction factor χ_{33} as a function of number of layers n and the relative elasticity modulus α

n	α					
	1	½	1/5	1/10	1/15	1/30
2	1.00	1.00	1.05	1.14	1.20	1.31
4	1.00	1.00	1.01	1.01	1.00	1.01
8	1.00	1.01	1.01	1.01	1.00	1.00
16	1.00	1.00	1.02	1.01	1.01	1.00
24	1.00	1.01	1.01	1.01	1.01	1.02
30	1.00	1.00	1.01	1.01	1.01	1.01
36	1.00	1.00	1.01	1.01	1.01	1.00

Table 7: Coupling correction factor χ_{34} as a function of even number of layers $n_{\parallel} = n_{\perp}$ and the relative elasticity modulus α

n	α					
	1	½	1/5	1/10	1/15	1/30
2	0.000	1.00	1.37	1.63	1.78	2.02
4	0.000	0.763	1.01	1.09	1.12	1.15
8	0.000	0.571	0.769	0.833	0.85	0.872
16	0.000	0.419	0.576	0.627	0.641	0.659
24	0.000	0.348	0.482	0.523	0.539	0.561
30	0.000	0.314	0.436	0.474	0.488	0.502
36	0.000	0.288	0.401	0.436	0.45	0.463

Table 8: Bending correction factor χ_{44} as a function of number of layers n and the relative elasticity modulus α

n	α					
	1	½	1/5	1/10	1/15	1/30
2	1.00	1.55	2.06	2.49	2.75	3.18
4	1.00	1.32	1.56	1.66	1.69	1.73
8	1.00	1.19	1.34	1.39	1.40	1.42
16	1.00	1.10	1.20	1.23	1.23	1.24
24	1.00	1.07	1.14	1.16	1.17	1.19
30	1.00	1.06	1.12	1.13	1.14	1.14
36	1.00	1.05	1.10	1.11	1.12	1.12

Table 9: Torsion correction factor χ_{66} as a function of number of layers n, the relative cross section height δ, and relative shear modulus γ

n	δ	γ				
		1	1/5	1/10	1/20	1/50
1	1	0.844	0.844	0.844	0.844	0.844
1	2	0.549	0.549	0.549	0.549	0.549
1	½	0.549	0.549	0.549	0.549	0.549
2	1	0.844	0.607	0.480	0.388	0.315
2	2	0.549	0.586	0.271	0.384	0.276
2	½	0.549	0.325	0.490	0.239	0.215
3	1	0.844	0.520	0.385	0.293	0.223
3	2	0.549	0.483	0.245	0.277	0.182
3	½	0.549	0.303	0.378	0.209	0.183
4	1	0.844	0.560	0.394	0.270	0.174
4	2	0.549	0.574	0.202	0.330	0.195

Continues on next page

Table of χ_{66} continues from previous page

n	δ	γ				
		1	1/5	1/10	1/20	1/50
4	½	0.549	0.278	0.460	0.154	0.118
7	1	0.844	0.519	0.343	0.215	0.118
7	2	0.549	0.531	0.163	0.284	0.153
7	½	0.549	0.249	0.413	0.110	0.073
8	1	0.844	0.541	0.358	0.223	0.117
8	2	0.549	0.569	0.161	0.310	0.167
8	½	0.549	0.251	0.449	0.104	0.064
15	1	0.844	0.526	0.340	0.203	0.097
15	2	0.549	0.550	0.144	0.293	0.151
15	½	0.549	0.240	0.429	0.084	0.043
16	1	0.844	0.535	0.347	0.223	0.098
16	2	0.549	0.568	0.145	0.310	0.158
16	½	0.549	0.241	0.446	0.085	0.042
21	1	0.844	0.527	0.341	0.201	0.094
21	2	0.549	0.555	0.141	0.295	0.152
21	½	0.549	0.238	0.433	0.080	0.038
24	1	0.844	0.534	0.345	0.204	0.094
24	2	0.549	0.568	0.142	0.304	0.156
24	½	0.549	0.239	0.445	0.080	0.037
30	1	0.844	0.533	0.345	0.203	0.093
30	2	0.549	0.568	0.140	0.303	0.156
30	½	0.549	0.238	0.445	0.079	0.036
31	1	0.844	0.529	0.341	0.201	0.092

Continues on next page

Table of χ_{66} continues from previous page

n	δ	γ				
		1	1/5	1/10	1/20	1/50
31	2	0.549	0.559	0.140	0.297	0.153
31	½	0.549	0.238	0.437	0.078	0.035
35	1	0.844	0.529	0.341	0.201	0.092
35	2	0.549	0.560	0.139	0.298	0.153
35	½	0.549	0.237	0.438	0.078	0.035
36	1	0.844	0.533	0.344	0.202	0.093
36	2	0.549	0.568	0.140	0.303	0.156
36	½	0.549	0.238	0.445	0.078	0.035

Table 10: Asymmetry correction factor χ^*_{33} as a function of number of layers n and relative elasticity modulus α

n	α					
	1	½	1/5	1/10	1/15	1/30
2	1	0.917	0.667	0.498	0.426	0.344
4	1	0.979	0.917	0.874	0.856	0.836
8	1	0.995	0.979	0.969	0.964	0.959
16	1	0.999	0.995	0.992	0.991	0.990
24	1	0.999	0.998	0.997	0.996	0.995
30	1	1.00	0.999	0.998	0.997	0.997
36	1	1.00	0.999	0.998	0.998	0.998

5.3 Stress correction factor

The maximum stress of the standard beam model and that of the refined model are compared and called the stress correction factor to get a picture about the

difference in the stress components. The stress correction factor

$$\psi_{ij}(\Xi) = \frac{\max_\Omega|\sigma_{ij}|}{\max_\Omega|\underline{\sigma}_\Xi|}, \qquad \Xi \in \{Q_x, Q_y, N, M_x, M_y, T\}, \tag{91}$$

is the other dependent variable of the simulation experiment. In the definition the maximum is over the cross section Ω. Stress correction factor quantifies the difference between the stress components by the standard and refined models when the cross section is loaded with the same stress resultants. The maximum stress of the refined model can be obtained by combination of the standard model maximum stress and the stress correction factor. The major stresses $\underline{\sigma}_\Xi$ for each loading mode are the ones that are non-zero in the standard model (see figure 6). Only the major stresses are taken into account in the measure although the refined model may predict other non-zero components. The major stress components are

$$\underline{\sigma}_{Q_x} = \underline{\sigma}_{zx}, \tag{92}$$

$$\underline{\sigma}_{Q_y} = \underline{\sigma}_{zy}, \tag{93}$$

$$\underline{\sigma}_N = \underline{\sigma}_{zz}, \tag{94}$$

$$\underline{\sigma}_{M_x} = \underline{\sigma}_{zz}, \tag{95}$$

$$\underline{\sigma}_{M_y} = \underline{\sigma}_{zz}, \tag{96}$$

$$\underline{\sigma}_T = \begin{cases} \underline{\sigma}_{zy}, & ij = zy \\ \underline{\sigma}_{zx}, & ij = zx \end{cases}. \tag{97}$$

Given the maximum stress of the cross section as predicted by the standard model, stress correction factor can be used to find the maximum stress of the refined model by

$$\max|\sigma_{ij}| = \max|\underline{\sigma}_\Xi|\psi_{ij}(\Xi)\,. \tag{98}$$

The independent variables affecting the stress correction factors are shown in table 11, in the same manner as table 4. The logical expressions in table 11 indicate whether the stress correction factors on the rows are affected by the independent variables on the columns. True means that the stress correction factor is affected by the independent variable, no matter what, and false that it is not affected. A logical expression defines the condition under which an independent variable affects a stress correction factor. Remarkable is that the stress correction factors for the loading by shear force Q_x, normal force N, as well as bending moments M_x, and M_y do not depend on the independent variables. Another important finding is that the relative Poisson's ratios are not inducing any difference in any of the stress correction factors.

The stress correction factors $\psi_{zy}(Q_y)$, $\psi_{zy}(T)$, $\psi_{zx}(T)$ obtained for the domains in table 3 are given in tables 12, 13, and 14. The stress correction factor for shear force Q_x is constant and found to be $\psi_{zx}(Q_x) = 1.5$, which is the same as the one found for an isotropic material (Freund and Karakoç, 2015; Timoshenko

Table 11: Stress correction factor dependencies of different loading cases for the independent parameters α, β, γ, and δ

Ξ(Mode)	factor	α	β	γ	δ	n
Q_x	ψ_{zx}	false	false	false	false	false
Q_y	ψ_{yz}	false	false	$n > 1$	false	$\gamma \neq 1$
N	ψ_z	false	false	false	false	false
M_x	ψ_z	false	false	false	false	false
M_y	ψ_z	false	false	false	false	false
T	ψ_{yz}	false	false	$n > 1$	true	$\gamma \neq 1$
	ψ_{zx}	false	false	$n > 1$	true	$\gamma \neq 1$

and Goodier, 1970). The stress correction factor ψ_{zy} for shear force loading Q_y presented in table 12 depends on the number of layers n and the relative shear modulus γ. The maximum value for $\psi_{zy}(\Xi = Q_y)$ was found to be 1.5 for a single layer beam and for isotropic material, minimum value 0.765 for even number of layers and $\gamma = 1/50$.

Stress correction factors for normal force N, bending moment M_x, and bending moment M_y were found to be equal to one.

The stress correction factor for shear stress $\tau_{yz}$for the shear load Q_y is given in table 12. For an odd number of layers, the values are decreasing with higher orthotropy and higher number of layers, except $n = 1$. The value decreases for higher orthotropy, but are unaffected of by the even number of layers. The error for the maximum major stresses for the loading modes of axial force and bending is found to vanish, $\psi(\Xi \in \{N, M_x, M_y\}) = 1$. Tables 13 and 14 presents the values of the stress correction factors for torsion load and the shear stresses τ_{yz} and τ_{zx}, respectively.

Table 12: Shear stress correction factor $\psi_{zy}(\Xi = Q_y)$ as a function of number of layers n and the relative shear modulus γ

n	γ				
	1	1/5	1/10	1/20	1/50
1	1.50	1.50	1.50	1.50	1.50
3	1.50	1.10	1.05	1.03	1.01
7	1.50	0.986	0.921	0.890	0.870
15	1.50	0.940	0.870	0.835	0.814
21	1.50	0.928	0.857	0.821	0.800
31	1.50	0.919	0.847	0.811	0.789
35	1.50	0.917	0.844	0.808	0.786
2	1.50	0.899	0.825	0.786	0.765
4	1.50	0.899	0.825	0.787	0.765
8	1.50	0.900	0.825	0.787	0.765
16	1.50	0.900	0.825	0.787	0.765
24	1.50	0.900	0.825	0.787	0.765
30	1.50	0.900	0.825	0.787	0.765
36	1.50	0.900	0.825	0.787	0.765

Table 13: Stress correction factor $\psi_{zy}(\Xi = T)$ as a function of number of layers n, the relative cross sectional height δ, and the relative shear modulus γ

n	δ	γ				
		1	1/5	1/10	1/20	1/50
1	1	1.58	1.58	1.58	1.58	1.58
1	2	1.31	1.31	1.31	1.31	1.31
1	½	3.37	3.37	3.37	3.37	3.37
2	1	1.58	1.59	1.83	2.12	2.47
2	2	1.32	0.931	0.997	1.15	1.46
2	½	3.35	4.57	5.26	5.84	6.36
3	1	1.58	1.43	1.59	2.00	2.44
3	2	1.33	0.893	0.900	1.16	1.53
3	½	3.36	3.82	4.39	4.90	5.38
4	1	1.58	1.49	1.64	2.08	2.72
4	2	1.33	0.878	0.830	1.02	1.36
4	½	3.35	4.28	5.10	5.99	7.06
7	1	1.59	1.38	1.47	1.84	2.55
7	2	1.33	0.853	0.790	0.922	1.20
7	½	3.37	3.75	4.40	5.33	6.75
8	1	1.58	1.32	1.32	1.64	2.31
8	2	1.31	0.802	0.720	0.807	1.01
8	½	3.36	3.61	4.19	5.15	6.87
15	1	1.59	1.22	1.21	1.29	1.62
15	2	1.32	0.760	0.700	0.690	0.772
15	½	3.36	3.25	3.62	4.38	6.22
16	1	1.59	1.20	1.17	1.24	1.53

Continues on next page

Table of $\psi_{zy}(\Xi = T)$ continues from previous page

n	δ	γ				
		1	1/5	1/10	1/20	1/50
16	2	1.32	0.740	0.670	0.650	0.714
16	½	3.37	3.15	3.39	3.99	5.59
21	1	1.59	1.20	1.17	1.23	1.54
21	2	1.33	0.751	0.670	0.643	0.671
21	½	3.36	3.13	3.33	3.87	5.58
24	1	1.59	1.18	1.14	1.17	1.42
24	2	1.32	0.729	0.650	0.611	0.624
24	½	3.38	3.10	3.27	3.78	5.27
30	1	1.59	1.16	1.11	1.12	1.29
30	2	1.32	0.722	0.640	0.590	0.578
30	½	3.37	2.98	3.04	3.36	4.39
31	1	1.59	1.17	1.11	1.12	1.29
31	2	1.34	0.731	0.640	0.599	0.586
31	½	3.39	3.00	3.06	3.36	4.37
35	1	1.59	1.16	1.10	1.09	1.22
35	2	1.32	0.728	0.640	0.591	0.571
35	½	3.38	2.97	3.00	3.25	4.14
36	1	1.59	1.15	1.09	1.08	1.19
36	2	1.32	0.718	0.630	0.580	0.557
36	½	3.39	2.96	2.99	3.23	4.10

Table 14: Stress correction factor $\psi_{zx}(\Xi = T)$ as a function of number of layers n, the relative cross sectional height δ, and the relative shear modulusγ

n	δ	γ				
		1	1/5		1/20	1/50
1	1	1.55	1.55	1.55	1.55	1.55
1	2	3.35	3.35	3.35	3.35	3.35
1	½	1.20	1.20	1.20	1.20	1.20
2	1	1.56	1.84	2.19	2.58	3.04
2	2	3.37	2.75	2.93	3.45	4.30
2	½	1.25	2.01	2.38	2.68	2.95
3	1	1.56	1.85	2.20	2.62	3.16
3	2	3.38	3.09	3.35	3.85	4.82
3	½	1.29	2.01	2.39	2.73	3.05
4	1	1.57	1.60	1.90	2.38	3.26
4	2	3.34	2.55	2.61	2.90	3.73
4	½	1.30	1.99	2.56	3.20	3.99
7	1	1.58	1.62	1.88	2.34	3.32
7	2	3.37	2.75	2.84	3.12	3.87
7	½	1.31	1.85	2.39	3.13	4.25
8	1	1.59	1.54	1.75	2.15	3.07
8	2	3.36	2.57	2.62	2.83	3.49
8	½	1.31	1.78	2.29	3.05	4.37
15	1	1.58	1.58	1.80	2.17	3.00
15	2	3.38	2.67	2.75	3.01	3.70
15	½	1.32	1.74	2.18	2.88	4.34
16	1	1.58	1.56	1.77	2.14	2.94

Continues on next page

Table of $\psi_{zx}(\Xi = T)$ continues from previous page

n	δ	γ				
		1	1/5	1/10	1/20	1/50
16	2	3.38	2.59	2.66	2.90	3.57
16	½	1.32	1.73	2.16	2.81	4.22
21	1	1.59	1.58	1.81	2.19	3.01
21	2	3.38	2.66	2.74	3.01	3.73
21	½	1.32	1.74	2.15	2.78	4.11
24	1	1.59	1.56	1.78	2.15	2.92
24	2	3.38	2.60	2.67	2.93	3.65
24	½	1.32	1.74	2.15	2.76	4.01
30	1	1.59	1.57	1.79	2.18	2.98
30	2	3.38	2.59	2.66	2.91	3.59
30	½	1.32	1.74	2.17	2.79	4.03
31	1	1.59	1.58	1.81	2.20	3.02
31	2	3.38	2.63	2.71	2.96	3.66
31	½	1.33	1.77	2.22	2.87	4.21
35	1	1.59	1.58	1.81	2.21	3.05
35	2	3.38	2.63	2.70	2.97	3.67
35	½	1.32	1.74	2.16	2.76	3.92
36	1	1.59	1.57	1.80	2.20	3.04
36	2	3.38	2.60	2.66	2.92	3.63
36	½	1.33	1.74	2.16	2.77	3.94

6 Modelling Error

In this chapter, the results of the simulations are analysed and discussed. The modelling error in rigidity is discussed in section 6.1 and the error in maximum stresses is discussed in section 6.2.

The figures contain also results for three layups called the t–series, which do not satisfy the equations (26) and (28). The aim is to give a picture about the effect of the stacking sequence. The t–series represents asymmetric plywood layups used by plywood industry. In addition to the standard s–series layups, the stacking sequences of the t–series plywood are given in Appendix 2 .

6.1 Modelling Error in Rigidity

The modelling error e in rigidity as predicted by the constitutive equation of the standard model is given by

$$e = ||\boldsymbol{\chi} - \boldsymbol{I}|| \leq |\chi_{11}-1|+|\chi_{22}-1|+|\chi_{33}-1|+|\chi_{44}-1|+|\chi_{55}-1|+|\chi_{66}-1|+2|\chi_{34}| \quad (99)$$

in which $\boldsymbol{I}$ is the 6 by 6 identity matrix and $||\,||$ is a matrix norm.

The error and its upper bound limit for a certain plywood can be calculated by using values of the rigidity correction factors obtained. By inserting the values of the rigidity correction factors in the upper bound of equation (99) the significant modes of the error can easily be seen. The error of a seven-layer plywood of birch material and a square cross section, is obtained by the values of the independent variables $\alpha = 1/15,\ \gamma = 1/5,\ \delta = 1$ and $n = 7$ by inserting the values into equation (99)

$$e = 0.581 \leq |-0.167| + |-0.581| + |0| + |0| + |0| + |-0.481| + 2|0| = 1.23, \quad (100)$$

using the L2–norm. Or for a 4 layered asymmetric birch plywood

$$e = 1.33 \leq |-0.167|+|-0.537|+|0|+|0.56|+|0|+|-0.606|+2|1.01| = 3.89. \quad (101)$$

The shear correction factor in the direction of the veneer is constant and found to be 5/6 for any cross stacked laminate of any orthotropic material. The result is the same as the well-known value for the shear correction factor for a rectangular cross section of isotropic material (Freund and Karakoç, 2015; Timoshenko et al., 1970). The shear correction factor $\chi_{11} = 5/6$ no matter the independent variables. The maximum value 5/6 of the shear correction factor χ_{22} is found for the single layer and for the isotropic equivalent material. The minimum value for χ_{22} is found for a highly orthotropic material $\gamma = 1/50$ and three layers. For the stretch correction factor χ_{33} the value is one for any value of the independent variables, except for a two-layer plywood where it increases to $\chi_{33} = 1.31$ for a highly orthotropic material for the relative elasticity modulus $\alpha = 1/30$. The coupling correction factor χ_{34} vanishes for any odd number of layers and when the relative elasticity modulus $\alpha = 1$. The maximum value $\chi_{34} = 2.02$ is found for a two-layer plywood of high orthotropy $\alpha = 1/30$. The value increases with a higher orthotropy and decreases

with a higher number of layers. Bending correction $\varkappa_{44}$ takes its minimum value 1, for the isotropic equivalent material and for all symmetric layups. The maximum value for $\varkappa_{44}$ is found for a highly orthotropic $\alpha = 1/30$ two-layer plywood, as 3.18. For even number of layers the value increases as the relative elasticity modulus α increases, and decreases with higher number of layers n. The bending correction factor $\varkappa_{55} = 1$, within the precision goal. The aspect ratio δ has a great impact on the torsion correction factor $\varkappa_{66}$. With a constant aspect ratio $\varkappa_{66}$ takes smaller values with an increasing orthotropy and increasing number of layers, except for aspect ratio $\delta = 2$. For aspect ratio $\delta = 2$ the values for odd number of layers gives values increasing for increasing number of layers , except for extremely high orthotropy $\gamma = 1/50$.

Figure shows 7 that the shear correction factor $\varkappa_{22}$ is independent of n for even number of layers, therefore it can be assumed that $\varkappa_{22}$ is dependent of the relation between longitudinal and transverse veneers $n_{\parallel}/n_{\perp}$ and the relative shear modulus γ. When the number of the longitudinal and the transverse plies are close to $n_{\parallel}/n_{\perp} \approx 1$ the value found for an even number of layers is a good reference. In addition, the asymmetry of any stacking sequence can be considered negligible, as the value is not changing by change in asymmetry (the even number line is constant with any number of layers). In the case of a usual five layer birch plywood, where the face layers are sanded to almost half of the initial thickness (Veistinen and Pennala, 1997) the cross sectional area of the longitudinal and the transverse layer are almost the same as for a four-layer equivalent plywood, with the parameters $\gamma = 1/5$. The value of the shear correction factor can be used as $\varkappa_{22} \approx 0.463$, for birch plywoods.

For highly asymmetric stacking sequences ($n = 2$) and clearly orthotropic material $\alpha \leq 1/2$ the error in rigidity for the loading mode M_x can be significant, but even for intermediate asymmetry $n = 4$ the error is vanishing, even for highly orthotropic materials $\alpha = 1/30$. The value of rigidity correction factor for N can be considered constant $\varkappa_{33} = 1$ for any produced plywood. Figure 11 that for symmetric layups with odd number of layers, the standard beam theory is predicting the rigidity correctly and therefore $\varkappa_{44} = 1$. The error of the the standard beam theory is negligible for the loading mode M_y and the rigidity factor $\varkappa_{55} = 1$.

For asymmetric layups the error is significant, and therefore it can be concluded that standard beam model is not predicting the rigidity for the highly orthotropic and highly asymmetric materials very well. Figure 11 shows that the error decreases rapidly as the asymmetry decreases (n increases).

The coupling factor $\varkappa_{34} = \varkappa_{43}$ for even number of layers is shown in figure 10. The coupling factor is decreasing decreases rapidly as the asymmetry decreases (n increases), but not as steep as $\varkappa_{44}$ in the interval for n of this thesis it is not seen to approach any single value.

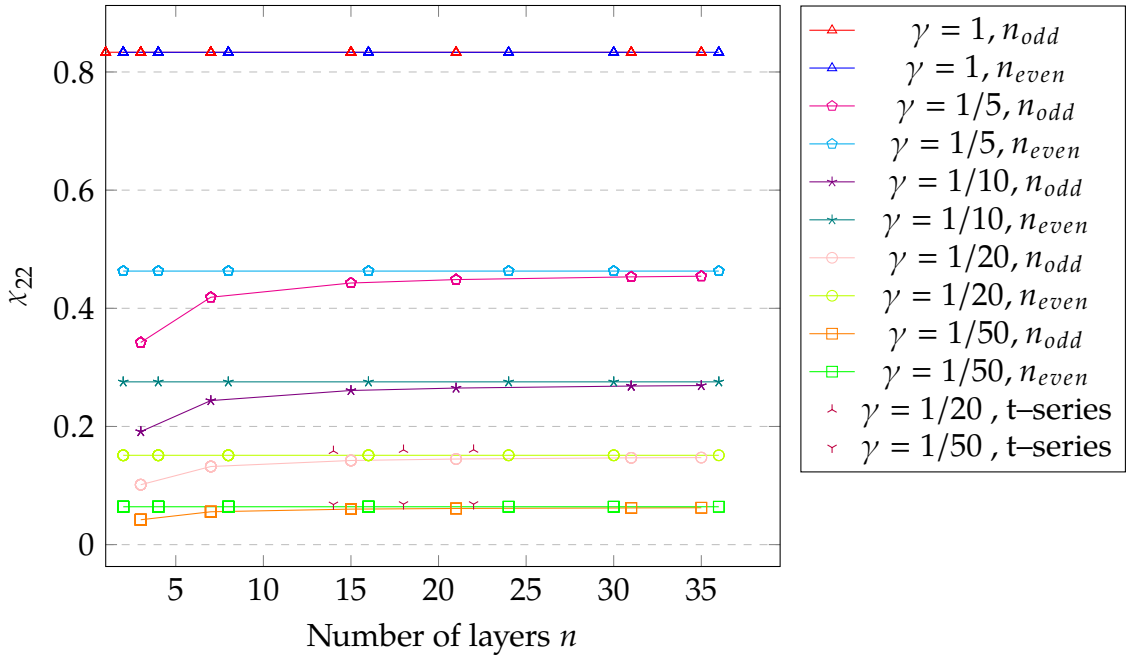

Figure 7: Shear correction factor χ_{22} for the loading mode of Q_y, for different values of γ

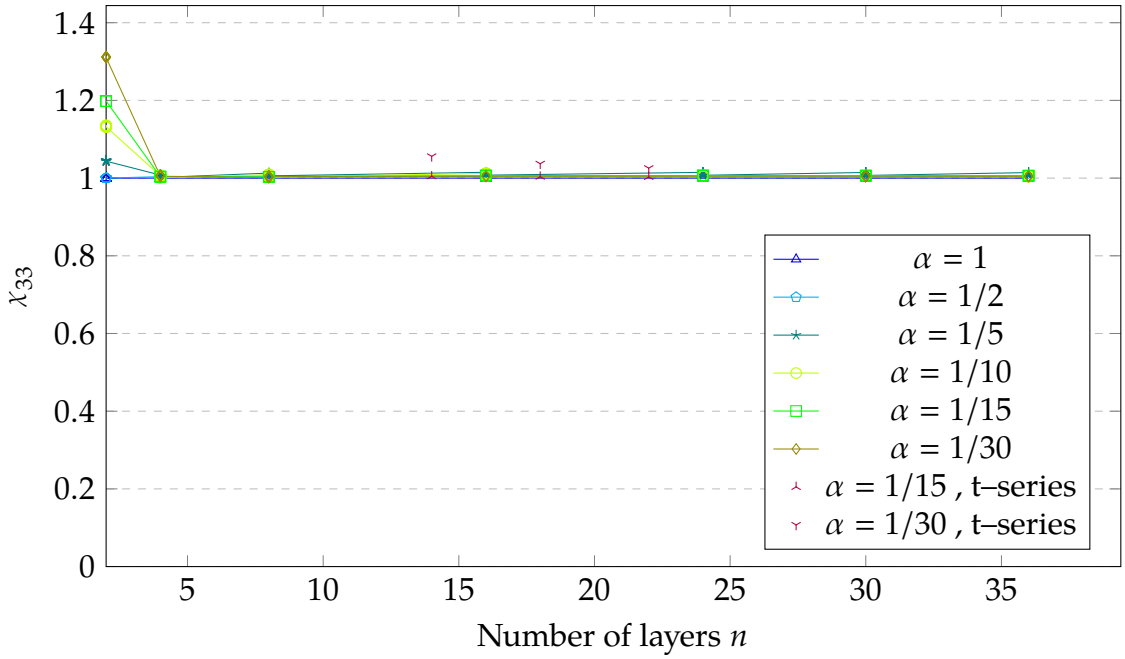

Figure 8: Rigidity correction factor χ_{33} for the loading mode of N, for different values of α

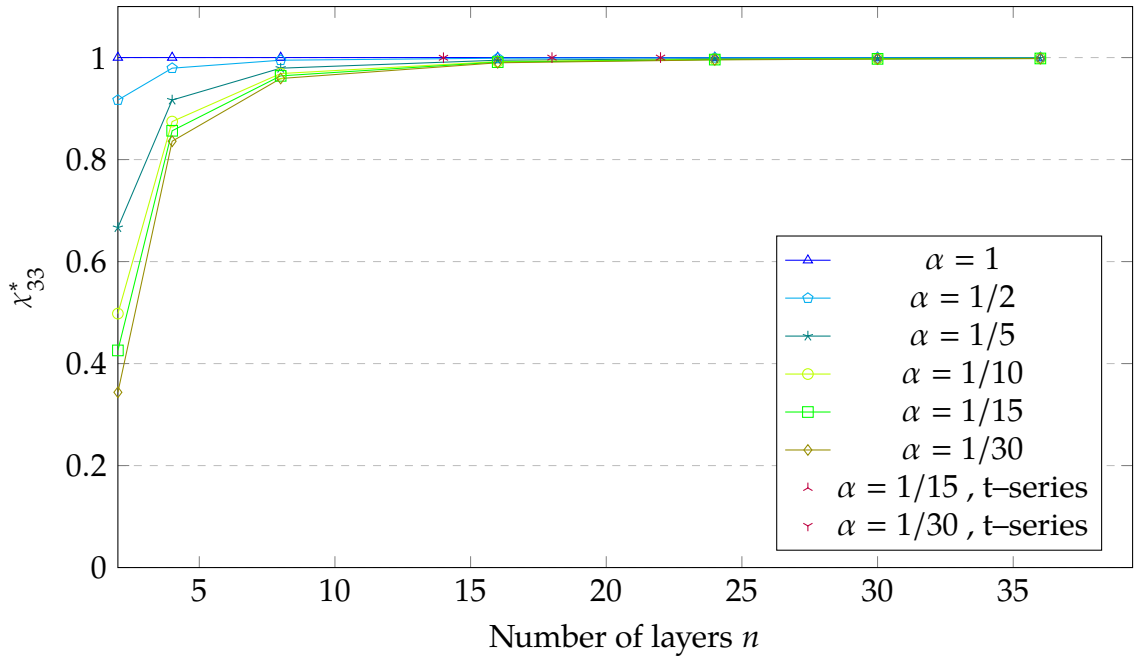

Figure 9: Correction factor, χ_{34} and χ_{43}, of coupling between the loading modes of N and M_x for different values of α

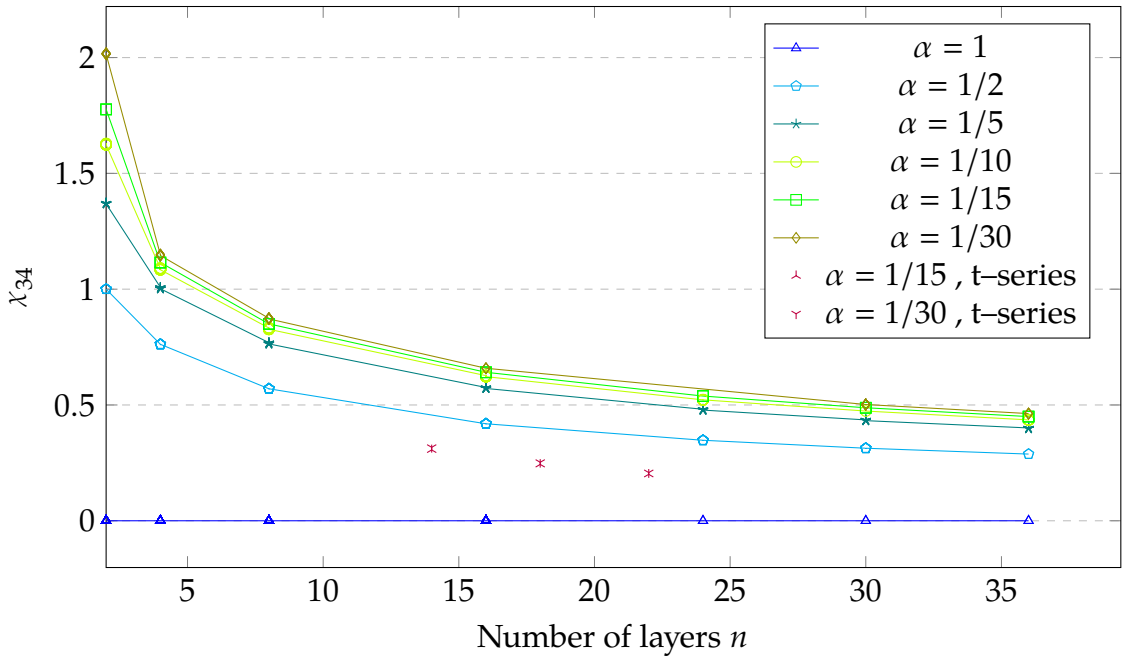

Figure 10: Correction factor, χ_{34} and χ_{43}, of coupling between the loading modes of N and M_x for different values of α

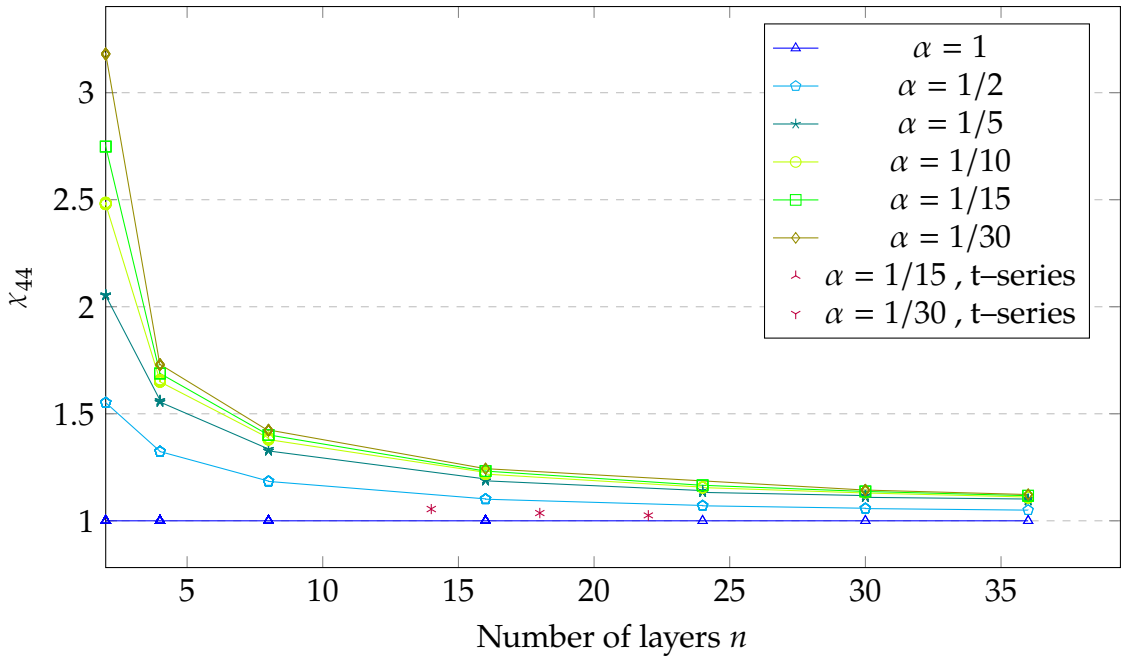

Figure 11: Rigidity correction factor χ_{44} for the loading mode of M_x, for different values of $\alpha$and even number of layers n

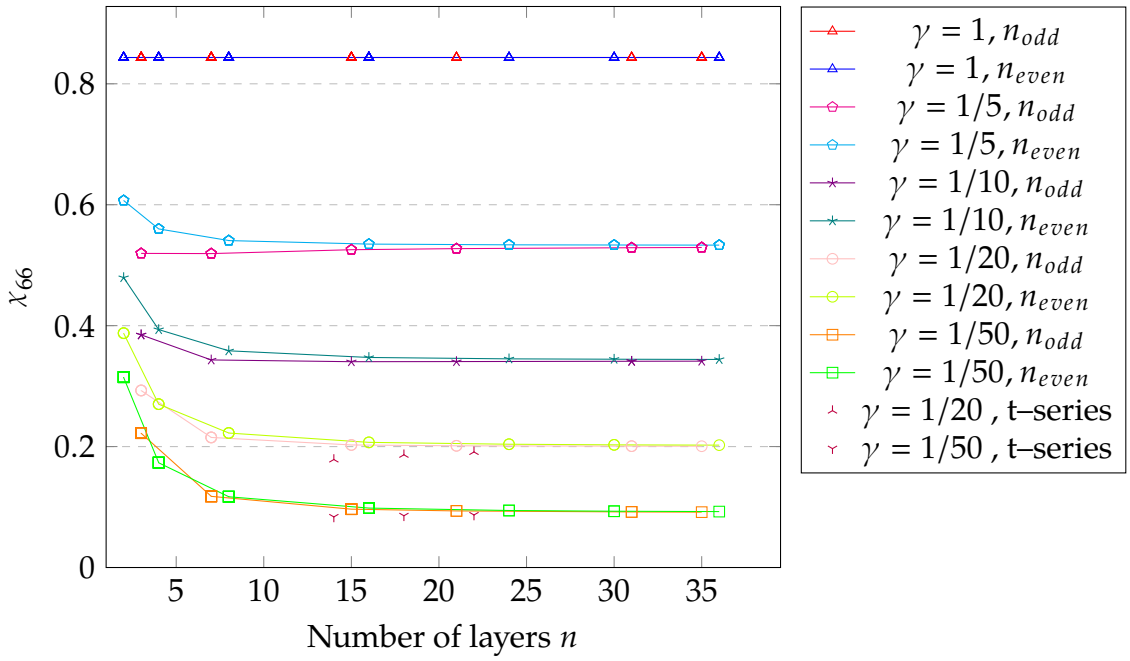

Figure 12: Rigidity correction factor χ_{66} for the loading mode of T, for $\delta = 1$ and values of γ

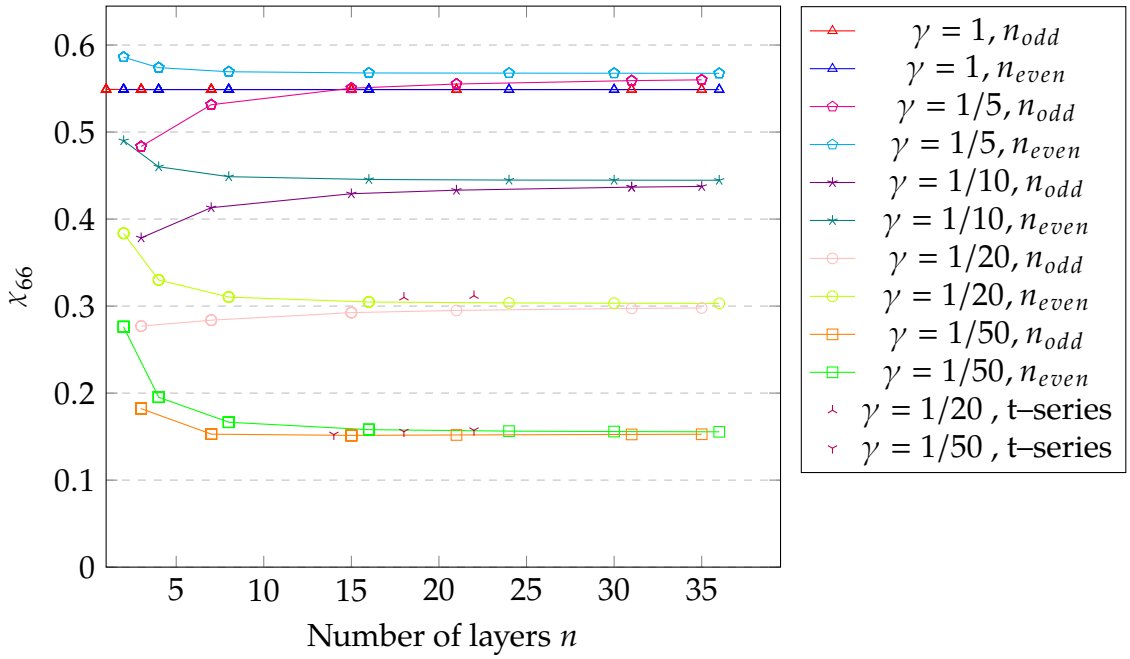

Figure 13: Rigidity correction factor χ_{66} for the loading mode of T, for $\delta = 2$ and values of γ

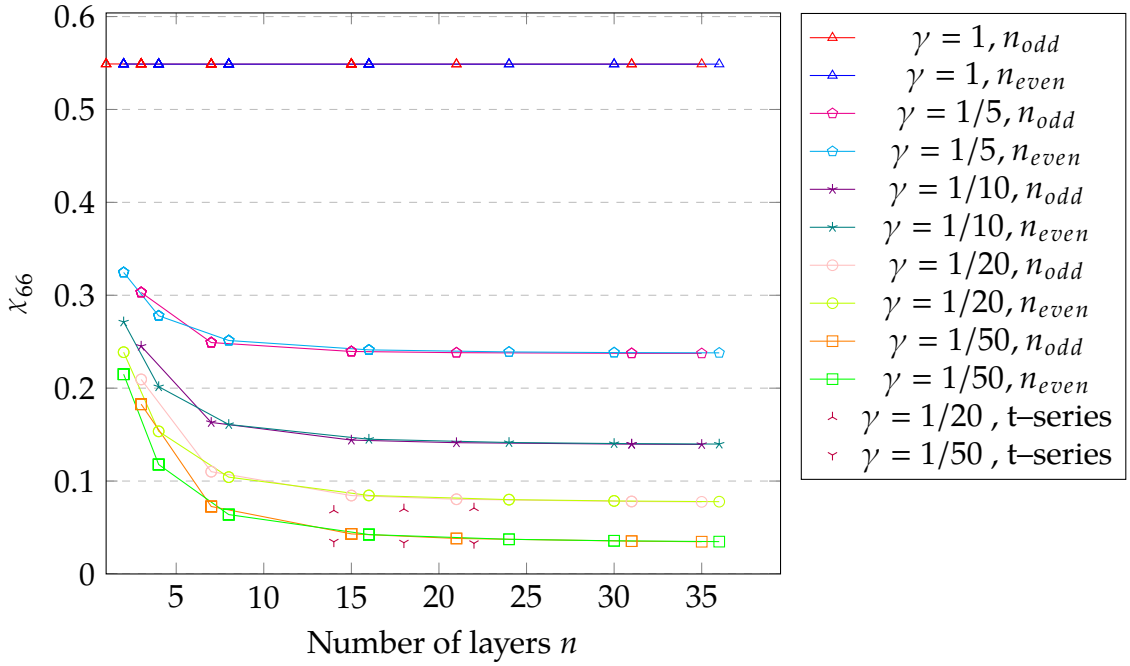

Figure 14: Rigidity correction factor χ_{66} for the loading mode of T, for $\delta = 1/2$ and values of γ

6.2 Modelling Error in Stress

In loading mode Q_x the stress correction factor shown in figure 15 is found not to dependent on the independent variables. The value 3/2 is the same as the well-known value for isotropic material found in literature (Timoshenko et al., 1970).

In loading mode Q_y, stress correction factor for stress component τ_{yz} shown in figure 7 is found to decrease as the orthotropic variable γ decreases, as shown in figure 7. The maximum value of the stress correction factor ψ_{yz} is found to be 3/2 (isotropic material). The minimum value 0.765 is found for a highly orthotropic material with an even number of layers. The stress correction factor for the t–series is very much below the s–series plywoods, which can be explained by the higher relative number of transverse layers. The relative number of transverse layers $n_\perp/n_\parallel$ of the t–series plywoods are 9/5, 11/7, and 13/9 which are all above the maximum one of the s–series plywoods.

In loading modes N, M_y, and M_x stress correction factor shown in figure 15 for stress component σ_{xx} is found to be independent of number of layers and material independent variables. The normal stress correction factor of ψxx for N, M_y, and M_x loading modes is close to one and can therefore be ignored. Figures 5 and 6 show that the standard beam model predicts also the stress distribution for the normal stress σ_{xx} correctly.

In loading mode T, stress correction factor for stress component τ_{zx} and for stress component τ_{yz} are depending on the relative shear modulus γ, the aspect ratio of the cross section δ, as well as the number of layers n. Figure 17 shows the stress correction factor for stress correction factor for stress component τ_{yz} for a square cross section, figure 19 for a high beam, and figure 18 for a wide beam. The value for an isotropic material is almost 1.59 for a square, 1.32 for a wide, and 3.39 for a high cross section. For high number of layers n the stress correction factor ψ_{zy} values are below the the values of the isotropic material ($\gamma = 1$), even for very orthotropic materials ($\gamma = 1/50$) for a square and a wide cross section. For a high cross section, the stress correction factor for τ_{yz}, orthotropic materials take values greater than for isotropic material for most plywood applications. For stress component τ_{zx} the stress correction factor seems to converge toward a single value for every simulated value of the relative shear modulus γ. The stress correction factor for stress component τ_{yz} the stress correction factor depends approximately only on the aspect ratio of the cross section δ and the relative shear modulus when the number of layers is higher than 15.

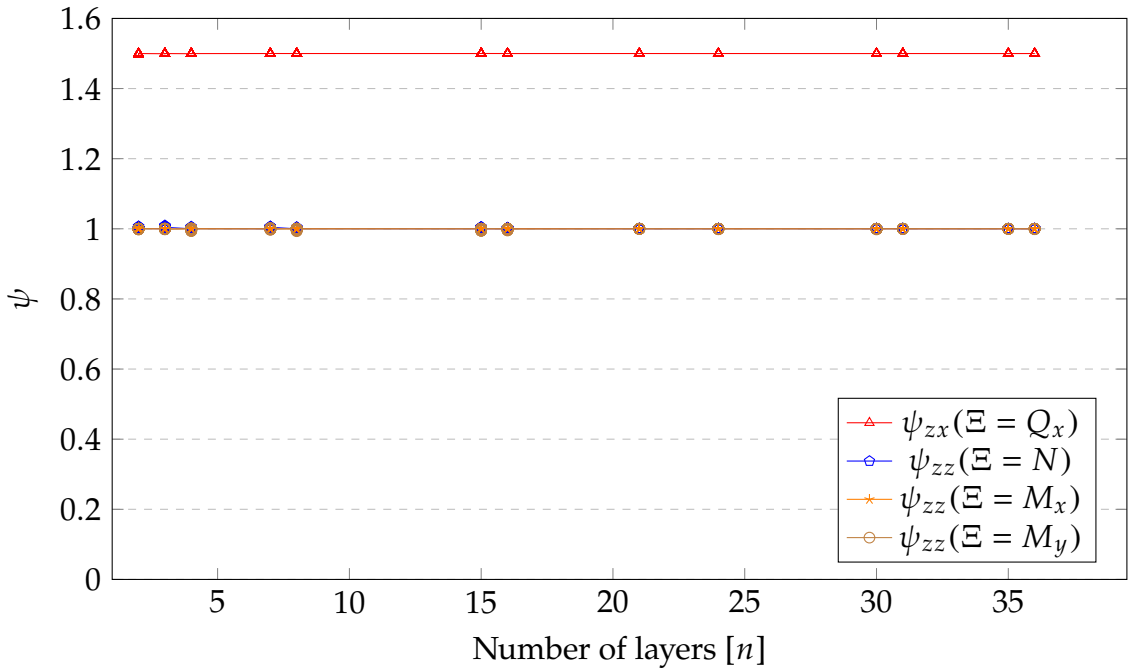

Figure 15: Stress correction factors for the loading modes of Q_x, N, M_x, and M_y

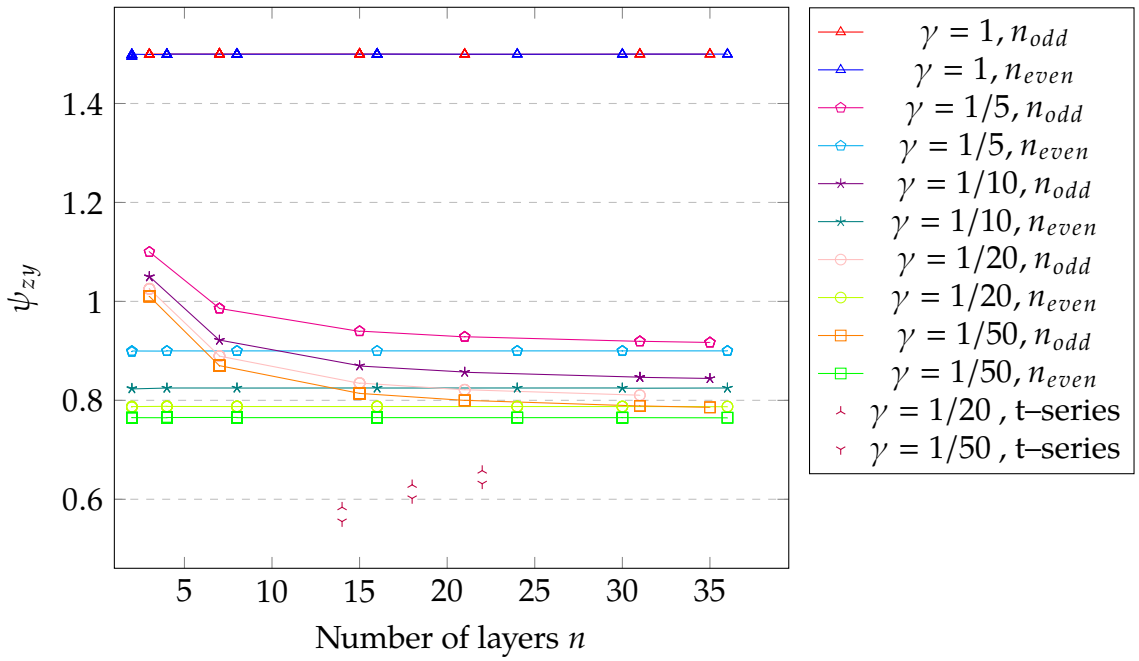

Figure 16: Shear stress correction factor for the loading mode of Q_y for different values of γ

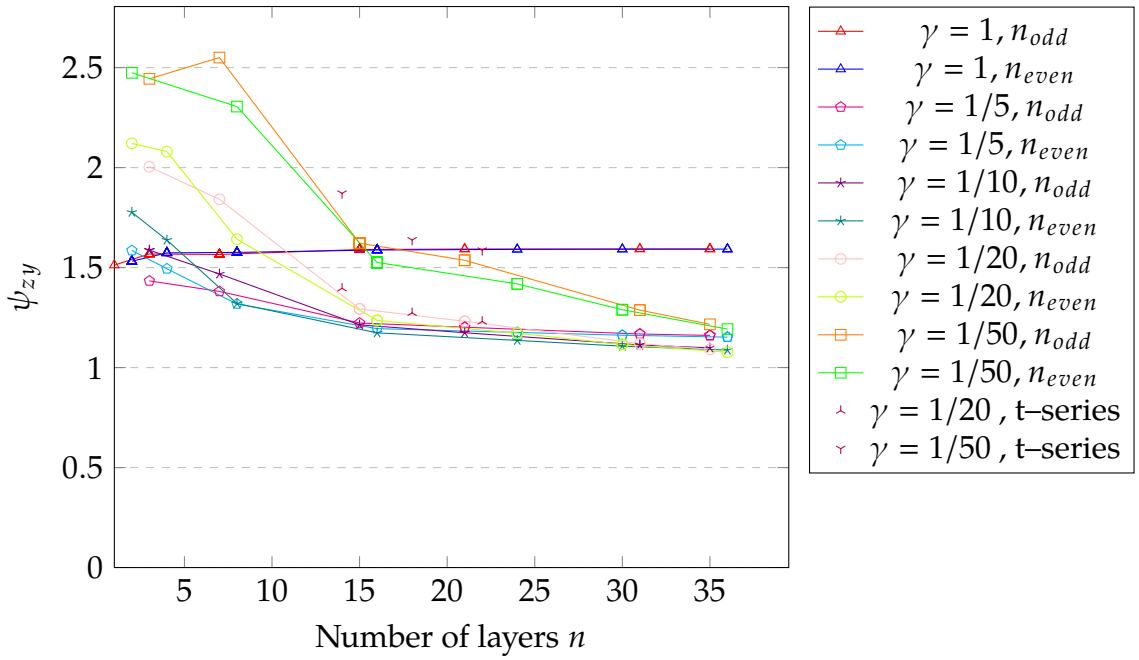

Figure 17: Shear stress correction factor ψ_{zy} for the loading mode of T, for $\delta = 1$ and values of γ

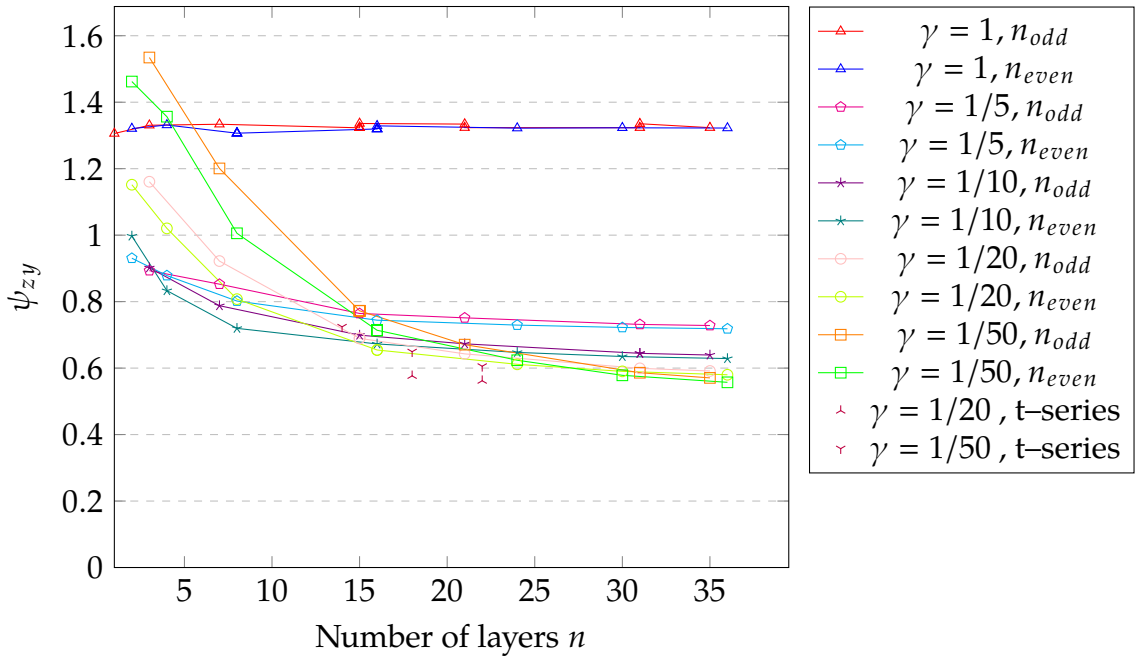

Figure 18: Shear stress correction factor ψ_{zy} for the loading mode of T, for $\delta = 2$ and values of γ

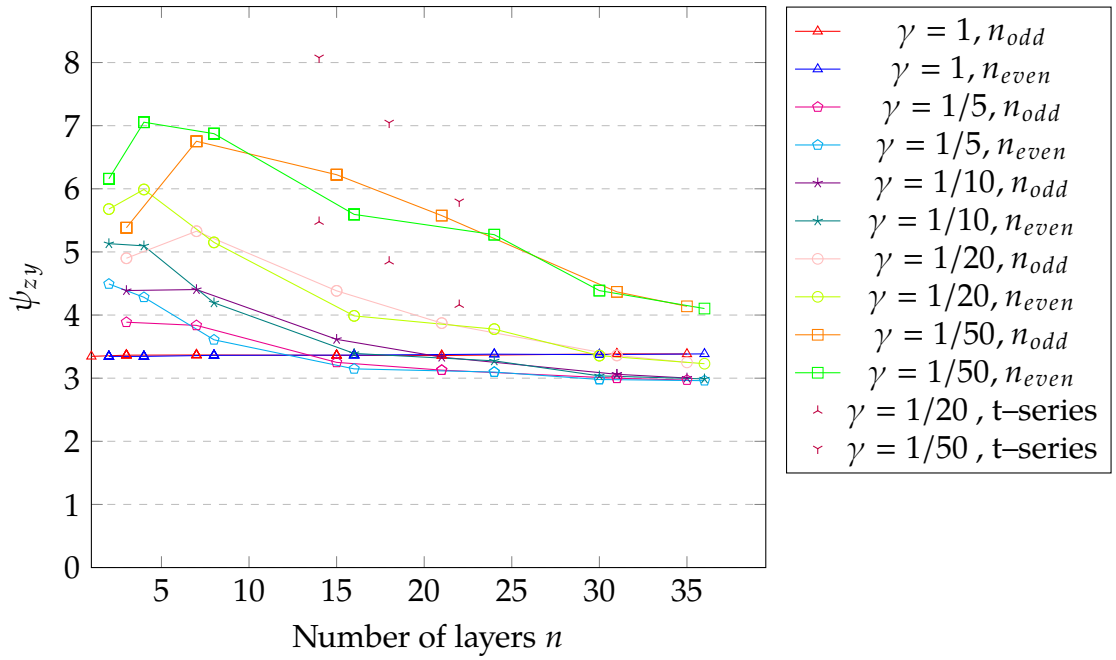

Figure 19: Shear stress correction factor ψ_{zy} for the loading mode of T, for $\delta = 1/2$ and values of γ

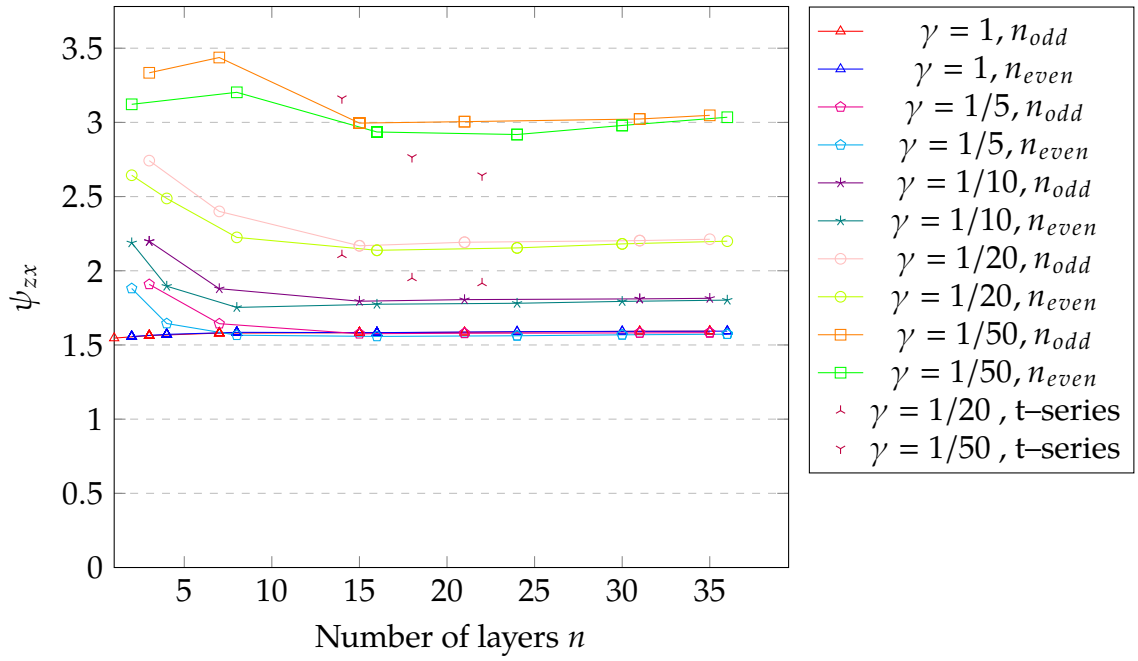

Figure 20: Shear stress correction factor ψ_{zx} for the loading mode of T, for $\delta = 1$ and values of γ

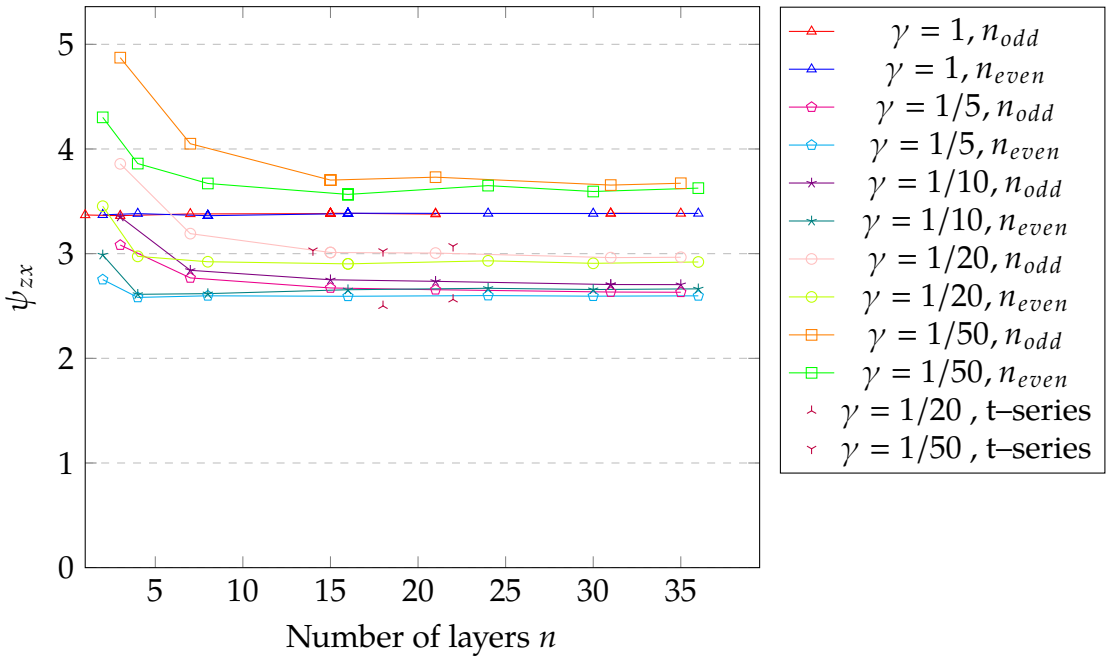

Figure 21: Shear stress correction factor ψ_{zx} for the loading mode of T, for $\delta = 2$ and values of γ

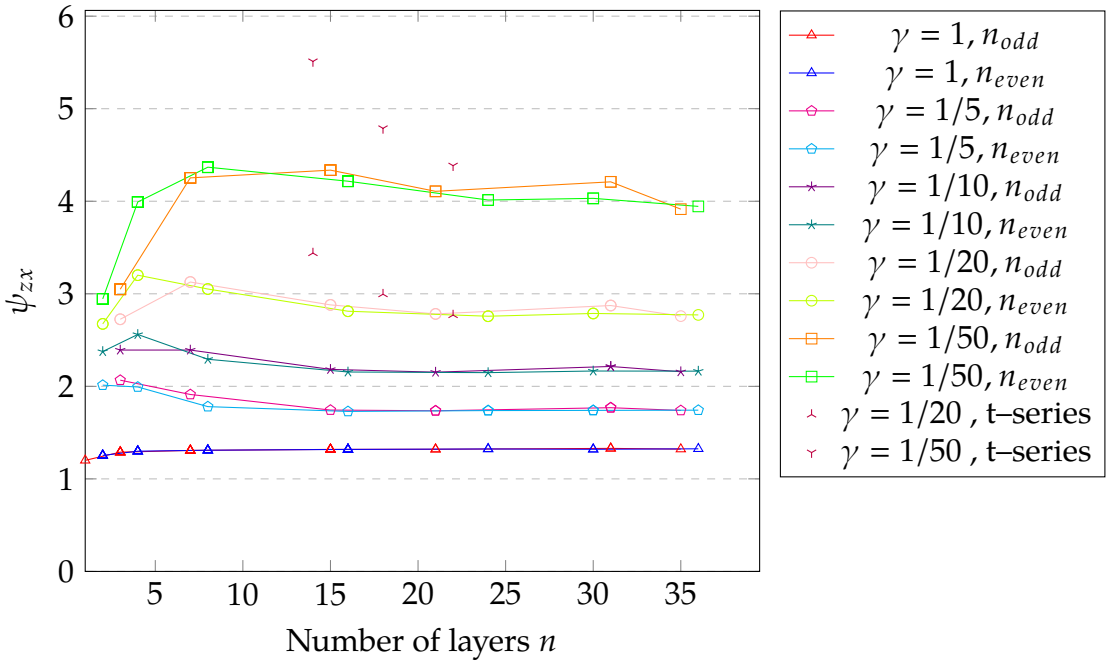

Figure 22: Shear stress correction factor ψ_{zx} for the loading mode of T, for $\delta = 1/2$ and values of γ

7 Discussion

The constitutive equations of the standard beam model and a refined beam model were compared to find the modelling error in the constitutive equation of the standard beam model. The underlying assumption of the comparison is that the modelling error in the refined model is much smaller than that of the standard one. A cross stacked plywood material with different values of relative material and geometric parameters were used in the comparison. The error was quantified by rigidity correction factors, which can be used to modify the constitutive equation of the standard beam model into the refined one. In stress, the error was quantified by comparing the maximum stress of the standard and refined models for each loading mode separately.

The rigidity correction factors indicate that the plywood beam constitutive equation of the standard model overestimates the rigidity in shear and torsion. However, the standard beam model predicts rigidity correctly in the stretching and bending modes, but underestimates the rigidity when the layup is highly asymmetric. For shear along the plies the standard model requires the well-known stress correction factor of 1.5 (Timoshenko et al., 1970). In the transverse direction to the plies the standard model stress is lower than 1.5 and even overestimated for most plywood applications. The standard model predicts the maximum normal stress correctly in bending and stretching modes. In torsion the modelling error in maximum shear stress is significant and is highly dependent on the aspect ratio and the orthotropy of the material. It is remarkable that none of the rigidity correction factors and neither any of the stress correction factors depends on the material variables for a single layer material, which is equivalent to a solid homogeneous orthotropic material. Therefore, the rigidity and stress correction factors results for isotropic material (Freund and Karakoç, 2015; Timoshenko et al., 1970), can be used for solid wood, for LVL with all veneers in the same direction, and Glulam beams.

As a conclusion, the standard model can be used to predict the rigidity of plywood beams for bending. In shear and torsion, the standard beam model may overestimate the rigidity by ten times and therefore, should not be trusted without a proper correction factor. The standard model can be used in strength based design of plywood beams when the shear is corrected by the well-known value 1.5 and in cases where torsion can be neglected.

For plywoods of more than seven layers the rigidity is predicted fairly well by the standard beam model using the material dependent rigidity correction factor of a plywood with even number of layers for the shear correction factor χ_{22}, 5/6 for shear correction factor χ_{11}, and the aspect ratio corrected torsion correction factor χ_{66} of a 16 layered plywood. In bending dominant loading cases the standard beam model shows no significant error. A special attention should be used in shear or torsion dominant cases, as the modelling error is significant, even for isotropic material. This may induce a significant error for certain boundary conditions, e.g., beams with clamped boundaries.

Finite element method with a non-structured mesh of quadratic elements

was used to solve the warping displacement of the refined beam model. The precision goal of this study was set to three significant figures. The values of the rigidity factors and the stress correction factors, except for torsion, were found to converge with 500 elements per layer for plywoods of less than 8 layers and with 100 elements per layer for larger number of layers. However, in some of the cases precision goal was not achieved within reasonable time due to the rather straightforward Mathematica implementation. Tuning of the in-house code may reduce the memory and the computing power required for the simulations.

Cross-stacked structure of identical plies was assumed in the study to reduce the number of geometrical and material parameters affecting the results. Structures consisting of layers of different thickness or several adjacent layers having the same orientation are also used in practice. Also plywood structures the veneer angles may differ from 0° and 90°, especially if other laminated composites are considered. Plywoods with a sandwich structures of different wood species or different material are used for aesthetics purposes, to gain in rigidity, or to get better insulation properties. The method of the present study applies also in these cases, but the correction factors need to be calculated case-by case.

The underlying assumption of the comparison is that the modelling error in the constitutive equation of the refined model is much smaller than that in the standard model. Although the concept of the modelling error always requires a baseline, the modelling error in the constitutive equation of the refined model compared to that obtained with stress given by the full elasticity theory would also be of interest. The uniform warping assumption was used to keep the simple form of the standard Timoshenko beam model and confine the effect of the warping displacement part into the constitutive equation only. The mechanical behaviour of a plywood beam close to boundaries should be studied to extend the understanding gained by this study. The constant rectangular cross section leaves open questions about different cross sections geometries and beams of non–constant cross section.

Bibliography

Cowper, G. R. (1968). "On the accuracy of Timoshenko's beam theory". *Journal of the Engineering Mechanics Division* 94.6, pp. 1447–1454.

El Fatmi, R. (2007). "Non-uniform warping including the effects of torsion and shear forces. Part I: A general beam theory". *International Journal of Solids and Structures* 44.18–19, pp. 5912 –5929. ISSN: 0020-7683. http://dx.doi.org/10.1016/j.ijsolstr.2007.02.006.

EN 310 (1993). *European Standard EN 310 Wood-based panels – Determination of modulus of elasticity in bending and bending strength*. Standard. European Committee for Standardization.

EN 338 (2003). *European Standard EN 338*. Standard. European Committee for Standardization.

EN 789 (2004). *European Standard EN 789 Timber structures - Test methods - Determination of mechanical properties of wood based panels*. Standard. European Committee for Standardization.

Puuinfo (2016). *Finnish Forest Industry, Statistics*. URL: https://www.forestindustries.fi/statistics/industry/25-Wood-Based\%20Panels\%20Industry/ (visited on 02/26/2016).

Freund, J. and Karakoç, A. (2015). "Shear and torsion correction factors of Timoshenko beam model for generic cross sections". *Engineering Structures & Materials* 2. http://dx.doi.org/10.17515/resm2015.19me0827.

Gere, J. and Timoshenko, S. (1984). *Mechanics of materials, 1984*. Chapman and Hall, London.

Gibson, L. J. and Ashby, M. F. (1997). *Cellular solids: structure and properties*. Cambridge university press.

Gould, P. L. (1994). *Introduction to linear elasticity*. Springer.

Hofstetter, K., Hellmich, C., and Eberhardsteiner, J. (2005). "Development and experimental validation of a continuum micromechanics model for the elasticity of wood". *European Journal of Mechanics - A/Solids* 24.6, pp. 1030 –1053. ISSN: 0997-7538. http://dx.doi.org/10.1016/j.euromechsol.2005.05.006.

Holmberg, S., Persson, K., and Petersson, H. (1999). "Nonlinear mechanical behaviour and analysis of wood and fibre materials". *Computers & Structures* 72.4–5, pp. 459 –480. ISSN: 0045-7949. http://dx.doi.org/10.1016/S0045-7949(98)00331-9.

Jr., L. M. and Qing, H. (2008). "Micromechanical modelling of mechanical behaviour and strength of wood: State-of-the-art review". *Computational Materials Science*

44.2, pp. 363 –370. ISSN: 0927-0256.
http://dx.doi.org/10.1016/j.commatsci.2008.03.043.

Kennedy, G. J. and Martins, J. R. (2012). "A homogenization-based theory for anisotropic beams with accurate through-section stress and strain prediction". *International Journal of Solids and Structures* 49.1, pp. 54 –72. ISSN: 0020-7683.
http://dx.doi.org/10.1016/j.ijsolstr.2011.09.012.

Kreyszig, E. (2006). *Advanced Engineering Mathematics*. 9th ed. John Wiley & Sons, Incorporated. ISBN: ISBN 978-0-471-48885-9.

Madabhusi-Raman, P. and Davalos, J. F. (1996). "Static shear correction factor for laminated rectangular beams". *Composites Part B: Engineering* 27.3–4. Structural Composites in Infrastructures, pp. 285 –293. ISSN: 1359-8368.
http://dx.doi.org/10.1016/1359-8368(95)00014-3.

Pai, P. F. (1995). "A new look at shear correction factors and warping functions of anisotropic laminates". *International Journal of Solids and Structures* 32.16, pp. 2295 –2313. ISSN: 0020-7683.
http://dx.doi.org/10.1016/0020-7683(94)00258-X.

Puuinfo (2016). *Puuinfo, Tuotteet*.
URL: http://www.puuinfo.fi/tuotteet (visited on 02/29/2016).

Qing, H. and Jr., L. M. (2011). "A 3D multilevel model of damage and strength of wood: Analysis of microstructural effects". *Mecha2011487nics of Materials* 43.9, pp. 487 –495. ISSN: 0167-6636.
http://dx.doi.org/10.1016/j.mechmat.2011.05.007.

Reddy, J., Wang, C., and Lee, K. (1997). "Relationships between bending solutions of classical and shear deformation beam theories". *International Journal of Solids and Structures* 34.26, pp. 3373 –3384. ISSN: 0020-7683.
http://dx.doi.org/10.1016/S0020-7683(96)00211-9.

Reddy, J. N. (2004). *Mechanics of laminated composite plates and shells: theory and analysis*. CRC press.

Schreurs, P. (2013). "Applied Elasticity in Engineering".
URL: http://www.mate.tue.nl/~piet/edu/ela/pdf/elasyl1213rev.pdf (visited on 03/23/2016).

Sjölund, J., Karakoç, A., and Freund, J. (2014). "Accuracy of regular wood cell structure model". *Mechanics of Materials* 76, pp. 35 –44. ISSN: 0167-6636.
http://dx.doi.org/10.1016/j.mechmat.2014.06.003.

Stephen, N. (1980). "Timoshenko's shear coefficient from a beam subjected to gravity loading". *Journal of Applied Mechanics* 47.1, pp. 121–127.

Timoshenko, S. and Goodier, J. (1970). *Theory of Elasticity*. McGraw-Hill, New York, NY.

Timoshenko, S., Goodier, J., and Abramson, H. N. (1970). "Theory of elasticity". *Journal of Applied Mechanics* 37, p. 888.

Timoshenko, S. P. (1921). "LXVI. On the correction for shear of the differential equation for transverse vibrations of prismatic bars". *The London, Edinburgh, and Dublin Philosophical Magazine and Journal of Science* 41.245, pp. 744–746.

— (1922). "X. On the transverse vibrations of bars of uniform cross-section". *Philosophical Magazine Series 6* 43.253, pp. 125–131. 10.1080/14786442208633855.

Veistinen, J. and Pennala, E. (1997). *Finnforest vanerikäsikirja*. Finnforest.

Wood Handbook (1999). *Wood Handbook: Wood as an Engineering Material*. United States Department of Agriculture, Forest Service.

Wood Solutions (2016). *Wood Solutions, design and build*. URL: https://www.woodsolutions.com.au/Wood-Product-Categories/ (visited on 03/17/2016).

Appendix 1 Elasticity Dyad Elements

The non – zero elements of the elasticity dyad is given by

$$\begin{aligned}
\underline{\underline{E}}_{xyxy} &= \underline{\underline{E}}_{xyyx} = \underline{\underline{E}}_{yxyx} = \underline{\underline{E}}_{yxxy} \\
&= G_{23}\cos^2\phi + G_{12}\sin^2\phi,
\end{aligned}$$

$$\begin{aligned}
\underline{\underline{E}}_{yzyz} &= \underline{\underline{E}}_{yzzy} = \underline{\underline{E}}_{zyzy} = \underline{\underline{E}}_{zyyz} \\
&= G_{23}\cos^2\phi + G_{12}\sin^2\phi,
\end{aligned}$$

$$\begin{aligned}
\underline{\underline{E}}_{xyyz} &= \underline{\underline{E}}_{xyzy} = \underline{\underline{E}}_{yxzy} = \underline{\underline{E}}_{yxyz} = \underline{\underline{E}}_{yzxy} = \underline{\underline{E}}_{zyxy} = \underline{\underline{E}}_{zyyx} = \underline{\underline{E}}_{yzyx} \\
&= (G_{23} - G_{12})\cos\phi\sin\phi,
\end{aligned}$$

$$\begin{aligned}
\underline{\underline{E}}_{xzxz} &= \underline{\underline{E}}_{xzzx} = \underline{\underline{E}}_{zxzx} = \underline{\underline{E}}_{zxxz} \\
&= \Big(- E_3 G_{31}(\nu_{13} - 3) + E_1(E_3 - G_{31}(\nu_{31} - 3)) + 4(E_1 - E_3)G_{31}\cos 2\phi \\
&\qquad + [E_3 G_{31}(1 + \nu_{31}) + E_1(-E_3 + G_{31}(1 + \nu_{31}))]\cos 4\phi\Big) / \\
&\quad \Big(4G_{31} + E_3(3 + \nu_{31}) - 4G_{31}\nu_{13}\nu_{31} + E_1(3 + \nu_{31}) + 4(E_1 - E_3)\cos 2\phi \\
&\qquad + (E_1 + E_3 - 4G_{31} - E_3\nu_{31} + 4G_{31}\nu_{31}\nu_{13})\cos 4\phi\Big),
\end{aligned}$$

$$\begin{aligned}
\underline{\underline{E}}_{xzzz} &= \underline{\underline{E}}_{zxzz} = \underline{\underline{E}}_{zzxz} = \underline{\underline{E}}_{zzzx} \\
&= \Big(4G_{31}(E_3(1 + \nu_{13}) - E_1(1 + \nu_{31}))\sin 2\phi \\
&\qquad - 2(E_3 G_{31}(1 + \nu_{13}) + E_1(-E_3 + G_{13} + G_{31}\nu_{31}))\sin 4\phi\Big) / \\
&\quad \Big(4G_{31} + E_3(3 + \nu_{13}) - 4G_{31}\nu_{13}\nu_{31} + E_1(3 + \nu_{31}) + 4(E_1 - E_3)\cos 2\phi \\
&\qquad + (E_1 + E_3 - 4G_{31} - E_3\nu_{13} - E_1\nu_{31} + 4G_{31}\nu_{13}\nu_{31})\cos 4\phi\Big),
\end{aligned}$$

$$\begin{aligned}
\underline{\underline{E}}_{zzzz} &= 4\Big(E_3 G_{31}(1 + \nu_{13}) + E_1(E_3 + G_{31} + G_{31}\nu_{31}) + \\
&\qquad [-E_3 G_{31}(1 + \nu_{31}) + E_1(E_3 - G_{31}(1 + \nu_{31}))]\cos 4\phi\Big) / \\
&\quad \Big(4G_{31} + E_3(3 + \nu_{13}) - 4G_{31}\nu_{13}\nu_{31} + E_1(3 + \nu_{31}) + 4(E_1 - E_3)\cos 2\phi \\
&\qquad + (E_1 + E_3 - 4G_{31} - E_3\nu_{13} - E_1\nu_{31} + 4G_{31}\nu_{13}\nu_{31})\cos 4\phi\Big).
\end{aligned}$$

Appendix 2 Stacking Sequences

Stacking sequence of simulated plywoods

n	Stacking sequence of s–series
1	|
2	| –
3	| – |
4	| – | –
7	| – | – | – |
8	| – | – | – | –
15	| – | – | – | – | – | – | – |
16	| – | – | – | – | – | – | – | –
21	| – | – | – | – | – | – | – | – | – | – |
24	| – | – | – | – | – | – | – | – | – | – | – | –
30	| – | – | – | – | – | – | – | – | – | – | – | – | – | – |
31	| – | – | – | – | – | – | – | – | – | – | – | – | – | – |
35	| – | – | – | – | – | – | – | – | – | – | – | – | – | – | – | – |
36	| – | – | – | – | – | – | – | – | – | – | – | – | – | – | – | – | – |
	Stacking sequence of t–series
14	| – – – | – | – – | – – – |
18	| – – – | – | – | – – | – | – – – |
22	| – – – | – | – | – | – – | – | – | – – – |

The notations used for the stacking sequences are | for a ply with grain direction to the axial direction of the beam, and – for a ply with the grain direction orthogonal to the axis of the beam. The normal notation for fibre reinforced composites are angles inside parentheses. Therefore the three layer standard plywood notations (0,90,0) and | – | are equivalent.